Lecture Notes on

NUMERICAL ANALYSIS of BIFURCATION PROBLEMS

Eusebius Doedel

Paris, November 2000

These are the notes for the "Numerical Continuation and Bifurcation Methods" lectures at the course on Bifurcation and Stability in Engineering, Paris, November 2000.

These notes and related documents and software are available by FTP from ftp.cs.concordia.ca. Log in as "anonymous" and give your full email address as password. Type "bin" (binary mode) before transferring any files. The following files are related to these lectures :

pub/doedel/doc/paris.ps.Z	these notes
pub/doedel/doc/hamburg.ps.Z	a more extensive set of notes
pub/doedel/auto/auto.ps.Z	the AUTO97 software reference manual
pub/doedel/auto/auto.tar.Z	the AUTO97 software package

Contents

1 Introduction

Numerical integrators can provide valuable insight into the transient behavior of a dynamical system. However, when the interest is in stationary and periodic solutions, their stability, and their transition to more complex behavior, then numerical continuation and bifurcation techniques are very powerful and efficient.

The objective of these lectures is to make every participant familiar with the ideas behind some basic numerical continuation and bifurcation techniques. This will be useful, and is at times necessary, for the effective use of the software AUTO and other packages, such as XPPAUT and CONTENT, that incorporate part of AUTO, as well as the new DDE-BIFTOOL, that has continuation capabilities for delay differential equations.

FTP site for AUTO:

ftp.cs.concordia.ca/pub/doedel/auto

FTP site for CONTENT:

ftp.cwi.nl/pub/CONTENT

Webpage DDE-BIFTOOL:

http://www.cs.kuleuven.ac.be/ koen/delay/ddebiftool.shtml

Webpage XPPAUT:

http://www.pitt.edu/~phase/

2 Regular Solutions

Consider a system of n equations in n unknowns $x \in \mathbf{R}^n$ and one free parameter $\lambda \in \mathbf{R}$:

$$G(x, \lambda) = 0, \qquad G(\cdot, \cdot) \in \mathbf{R}^n.$$

Let $X \equiv (x, \lambda)$. Then the equation can be written

$$G(X) = 0, \qquad G : \mathbf{R}^{n+1} \to \mathbf{R}^n.$$

A solution X_0 of $G(X) = 0$ is called a *regular solution* if the Jacobian matrix $G_X^0 \equiv G_X(X_0)$ has maximal rank, i.e., if $\mathrm{Rank}(G_X^0) = n$. This means that the n rows of G_X^0 are linearly independent. Equivalently, it means that G_X^0 has n linearly independent columns. (Note that the matrix $G_X^0 \equiv (G_x^0 \mid G_\lambda^0)$ has n rows and $n+1$ columns.)

If $X_0 \equiv (x_0, \lambda_0)$ is a regular solution of $G(X) = 0$ then near X_0, there exists a unique one-dimensional continuum of solutions $X(s)$ with $X(0) = X_0$.

REMARKS 1) Such a continuum of solutions is referred to as a *solution branch*. 2) If the Jacobian matrix G_x^0 is nonsingular then $X_0 \equiv (x_0, \lambda_0)$ is regular. In this case the solution x is locally a function of λ, as follow from the "Implicit Function Theorem". 3) A generic "fold" (or saddle-node) is also regular solution!

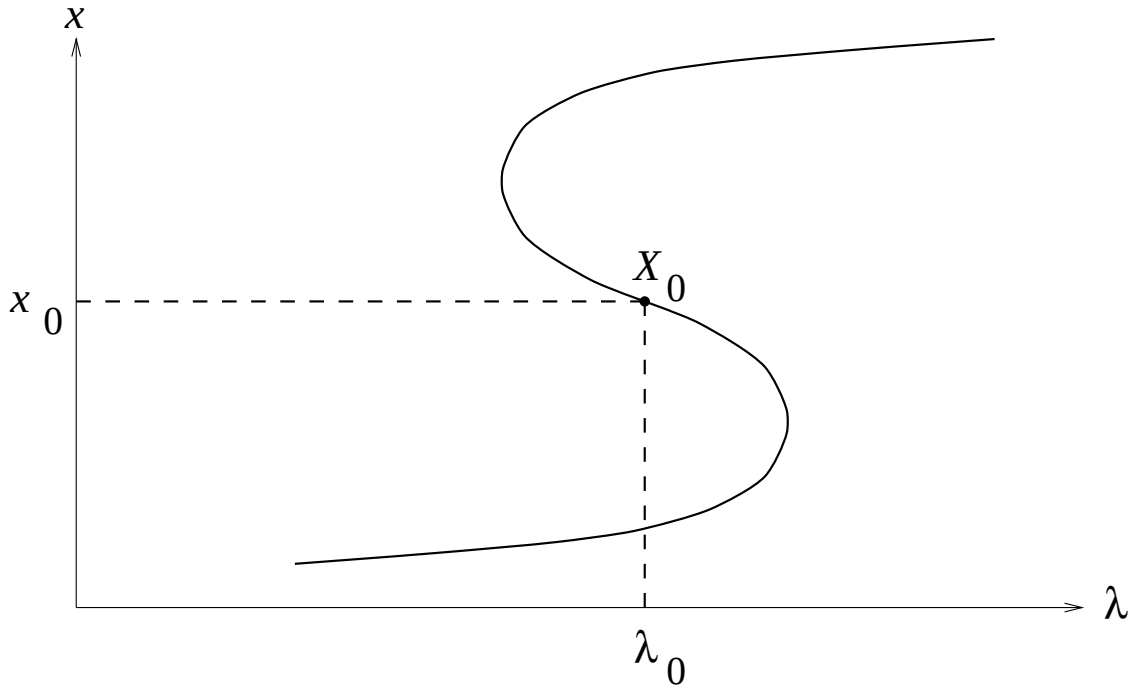

Figure 1: A solution branch of $G(x, \lambda) = 0$. Note the two folds.

3 Example : A Predator-Prey Model

$$\begin{cases} x_1' = & 3x_1(1-x_1) - x_1x_2 - \lambda(1 - e^{-5x_1}), \\ x_2' = & -x_2 + 3x_1x_2. \end{cases}$$

Here x_1 may be thought of as "fish" and x_2 as "sharks", while the term $\lambda(1 - e^{-5x_1})$ represents "fishing", with "fishing-quota" λ.

When $\lambda = 0$ the *stationary solutions* are

$$\left.\begin{array}{ll} 3x_1(1-x_1) - x_1x_2 & = 0 \\ -x_2 + 3x_1x_2 & = 0 \end{array}\right\} \Rightarrow (x_1, x_2) \;=\; (0,0), \quad (1,0), \quad (\frac{1}{3}, 2).$$

The Jacobian matrix is

$$J(x_1, x_2; \lambda) \equiv \begin{pmatrix} 3 - 6x_1 - x_2 - 5\lambda e^{5x_1} & -x_1 \\ 3x_2 & -1 + 3x_1 \end{pmatrix}$$

In particular,

$$J(0,0;0) = \begin{pmatrix} 3 & 0 \\ 0 & -1 \end{pmatrix}; \qquad \text{eigenvalues 3, -1} \quad \text{(unstable)}$$

$$J(1,0;0) = \begin{pmatrix} -3 & -1 \\ 0 & 2 \end{pmatrix}; \qquad \text{eigenvalues -3, 2} \quad \text{(unstable)}$$

$$J(\frac{1}{3},2;0) = \begin{pmatrix} -1 & -\frac{1}{3} \\ 6 & 0 \end{pmatrix}; \qquad \text{eigenvalues } -\tfrac{1}{2} \pm \tfrac{1}{2}i\sqrt{7} \quad \text{(stable)}$$

Note that all three Jacobians at $\lambda = 0$ are nonsingular. So all three stationary points give rise to a solution branch.

In this problem we can *explicitly* find all solutions:

I :

$$(x_1, x_2) = (0,0).$$

II :

$$x_2 = 0, \qquad \lambda = \frac{3x_1(1-x_1)}{1-e^{-5x_1}} \ . \qquad \Big(\text{Note that } \lim_{x_1 \to 0} \frac{3(1-2x_1)}{5e^{-5x_1}} = \frac{3}{5} \ .\Big)$$

III :

$$x_1 = \frac{1}{3}, \qquad \frac{2}{3} - \frac{1}{3}\, x_2 - \lambda(1-e^{-5/3}) = 0 \ \Rightarrow \ x_2 = 2 - 3\lambda(1-e^{-5/3}).$$

These *solution branches* intersect at two *branch points*, one being $(x_1, x_2, \lambda) = (0, 0, 3/5)$.

Stability of branch I :

$$J(0,0;\lambda) = \begin{pmatrix} 3-5\lambda & 0 \\ 0 & -1 \end{pmatrix}; \qquad \text{eigenvalues } \ 3-5\lambda, \ \ -1.$$

So the zero solution is unstable if $\lambda < 3/5$, and stable if $\lambda > 3/5$.

Stability of branch II : This branch has no stable positive solutions.

Stability of branch III : At $\lambda_H \approx 0.67$ the complex eigenvalues cross the imaginary axis. This crossing is a *Hopf bifurcation*. Beyond λ_H there are *periodic solutions* whose period T increases as λ increases. The period becomes infinite at $\lambda = \lambda_\infty \approx 0.7$. This final orbit is, in fact, a *heteroclinic cycle*.

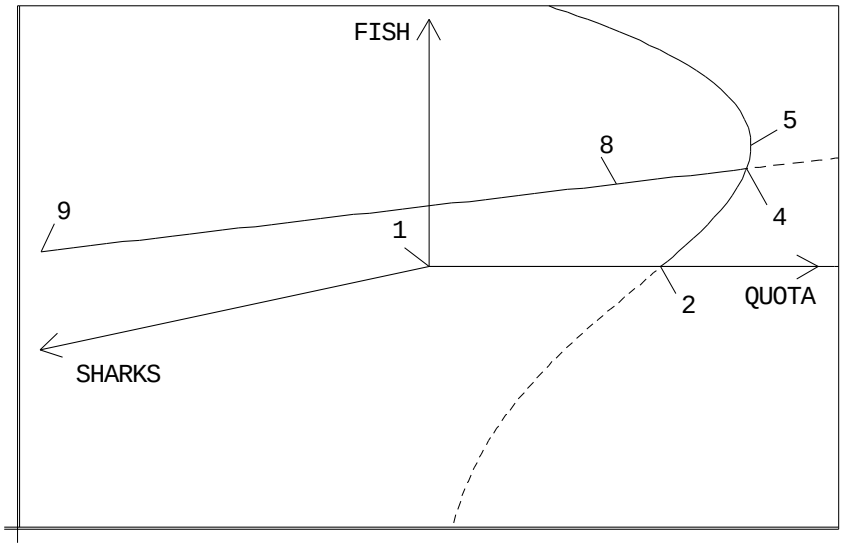

Figure 2: Stationary solution branches of the predator-prey model. Solutions 2 and 4 are branch points. Solution 8 is a Hopf bifurcation point.

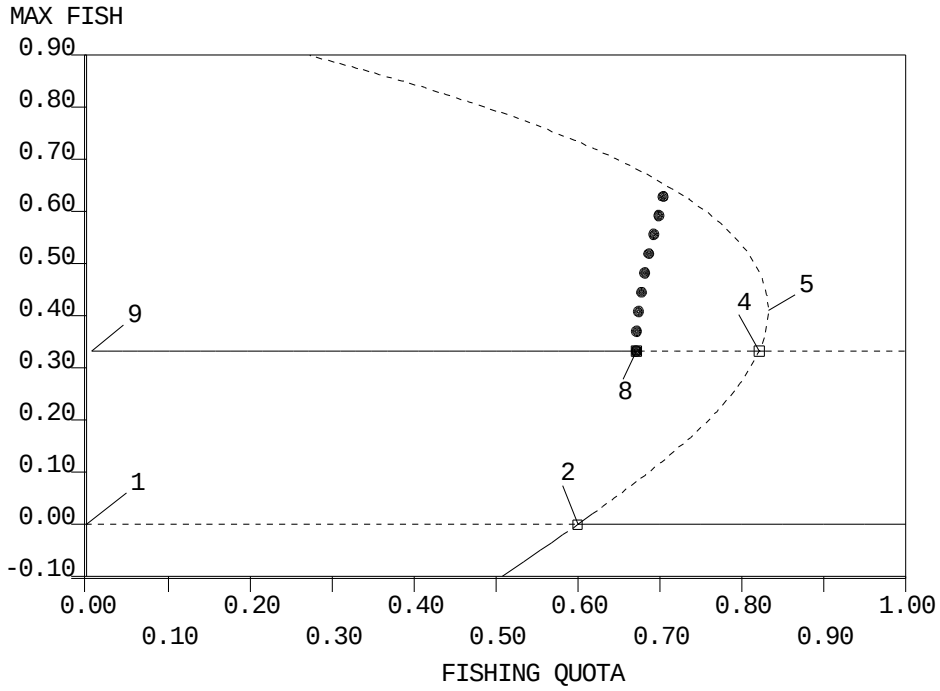

Figure 3: Bifurcation diagram of the predator-prey model. The periodic solution branch is also shown. For stationary solutions the vertical axis is simply x_1, while for periodic solutions $max\ x_1$ is plotted. Solid/dashed lines denote stable/unstable solution. Open squares are branch points; the solid square is a Hopf bifurcation.

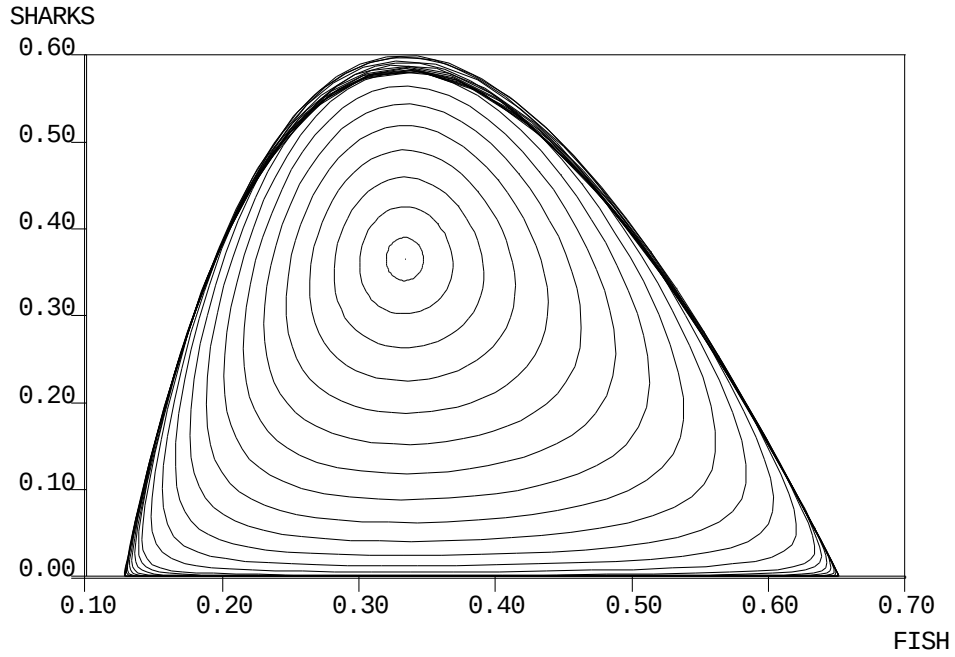

Figure 4: Some periodic solutions of the predator-prey model. The final orbit is very close to a heteroclinic cycle.

From Figure 3 we can deduce the solution behavior for (slowly) increasing λ :

- Branch III is followed until λ_H.
- Periodic solutions of increasing period until $\lambda = \lambda_\infty$.
- Collapse to trivial solution (Branch I).

EXERCISE. Use AUTO to repeat these calculations. (Execute Run 1 and Run 3 of demo `pp2`.)

4 Newton's Method

Recall Newton's method for finding a solution of the scalar equation $f(x) = 0$:

$$x^{(\nu+1)} = x^{(\nu)} - \frac{f(x^{(\nu)})}{f_x(x^{(\nu)})}, \qquad \nu = 0, 1, 2, \cdots, \qquad x^{(0)} \text{ given.}$$

This can be rewritten as

$$f_x(x^{(\nu)})(x^{(\nu+1)} - x^{(\nu)}) = -f(x^{(\nu)}),$$

or

$$f_x(x^{(\nu)})\Delta x^{(\nu)} = -f(x^{(\nu)}),$$

where $\Delta x^{(\nu)} \equiv x^{(\nu+1)} - x^{(\nu)}$, so that

$$x^{(\nu+1)} = x^{(\nu)} + \Delta x^{(\nu)}.$$

This last formulation can also be used for systems of equations

$$G(x) = 0, \qquad G \ : \ \mathbf{R}^n \to \mathbf{R}^n.$$

Solving $G(x) = 0$ by Newton's method takes the form

$$G_x(x^{(\nu)})\Delta x^{(\nu)} = -G(x^{(\nu)}),$$

$$x^{(\nu+1)} = x^{(\nu)} + \Delta x^{(\nu)}.$$

Here the Jacobian matrix $G_x(\cdot)$ is a square matrix.

5 Parameter Continuation

Suppose we have a solution (x_0, λ_0) of

$$G(x, \lambda) = 0,$$

as well as the direction vector $\dot{x}_0$. Here $\dot{x} \equiv dx/d\lambda$. We want to compute the solution x_1 at $\lambda_1 \equiv \lambda_0 + \Delta\lambda$.

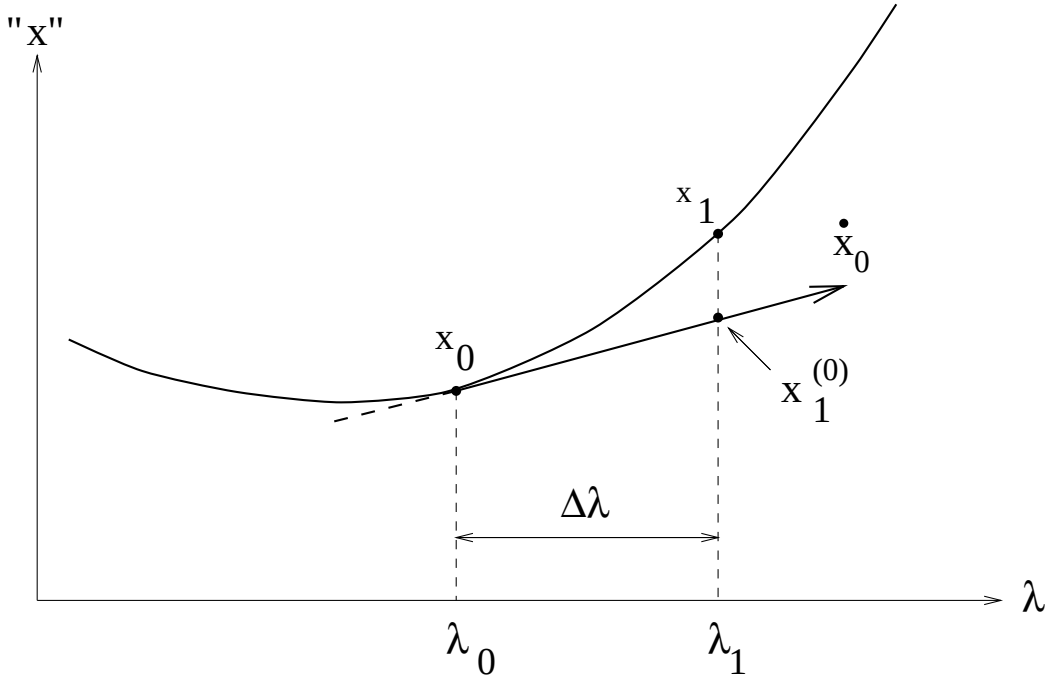

Figure 5: Graphical interpretation of parameter continuation.

To find the solution x_1 we use Newton's method

$$G_x(x_1^{(\nu)}, \lambda_1)\ \Delta x_1^{(\nu)} = -G(x_1^{(\nu)}, \lambda_1) \qquad \nu = 0, 1, 2, \cdots.$$

$$x_1^{(\nu+1)} = x_1^{(\nu)} + \Delta x_1^{(\nu)}.$$

Take

$$x_1^{(0)} = x_0 + \Delta\lambda\ \dot{x}_0.$$

If $G_x(x_1, \lambda_1)$ is nonsingular and $\Delta\lambda$ sufficiently small then the convergence theory for Newton's method assures that this iteration will converge.

After convergence, the new direction $\dot{x}_1$ can be obtained by solving

$$G_x(x_1, \lambda_1)\dot{x}_1 = -G_\lambda(x_1, \lambda_1).$$

This equation follows from differentiating $G(x(\lambda), \lambda) = 0$ with respect to λ at $\lambda = \lambda_1$.

6 Example : The Bratu Problem

$$x''(t) + \lambda e^{x(t)} = 0 \quad \text{for} \quad t \in [0, 1], \qquad x(0) = 0, \qquad x(1) = 0.$$

Note that if $\lambda = 0$ then $x(t) \equiv 0$ is a solution.

Discretize by introducing a mesh,

$$\{0 = t_0 < t_1 < \cdots < t_N = 1\}, \qquad t_j - t_{j-1} = h, \quad (1 \le j \le N), \qquad h = 1/N.$$

The discrete equations are :

$$\frac{x^{j+1} - 2x^j + x^{j-1}}{h^2} + \lambda e^{x^j} = 0, \qquad j = 1, \cdots, N-1,$$

with $x^0 = x^N = 0$.

Let

$$x \equiv (x^1, x^2, \cdots, x^{N-1}).$$

Then we can write the above as

$$G(x, \lambda) = 0,$$

where

$$G \ : \ \mathbf{R}^n \times \mathbf{R} \to \mathbf{R}^n, \qquad n \equiv N - 1.$$

Parameter continuation : Suppose we have λ_0, x_0 and $\dot{x}_0$. Set

$$\lambda_1 = \lambda_0 + \Delta\lambda.$$

Newton's method :

$$\begin{aligned} G_x(x_1^{(\nu)}, \lambda_1)\Delta x_1^{(\nu)} &= -G(x_1^{(\nu)}, \lambda_1) \\ x_1^{(\nu+1)} &= x_1^{(\nu)} + \Delta x_1^{(\nu)} \end{aligned} \qquad \nu = 0, 1, 2, \cdots,$$

with $x_1^{(0)} = x_0 + \Delta\lambda\dot{x}_0$. After convergence find $\dot{x}_1$ from

$$G_x(x_1, \lambda_1)\dot{x}_1 = -G_\lambda(x_1, \lambda_1).$$

Repeat the procedure to find x_2, x_3, x_4, $\cdots$.

Above

$$G_x(x,\lambda) = \begin{pmatrix} -\frac{2}{h^2} + \lambda e^{x^1} & \frac{1}{h^2} & & \\ \frac{1}{h^2} & -\frac{2}{h^2} + \lambda e^{x^2} & \frac{1}{h^2} & \\ & \cdot & \cdot & \cdot \\ & & \frac{1}{h^2} & -\frac{2}{h^2} + \lambda e^{x^{N-1}} \end{pmatrix}.$$

Thus we must solve a tridiagonal system for each Newton iteration.

Actually, AUTO does not use finite differences as discretization. AUTO uses orthogonal collocation with piecewise polynomials, to be discussed later.

EXERCISE. Use AUTO demo `exp` to compute the solution branch of Bratu's equation. Plot the bifurcation diagram and some solutions. Note that the solution branch contains a fold. The parameter continuation method would fail at such a point. Indeed, AUTO uses the pseudo-arclength continuation method introduced below.

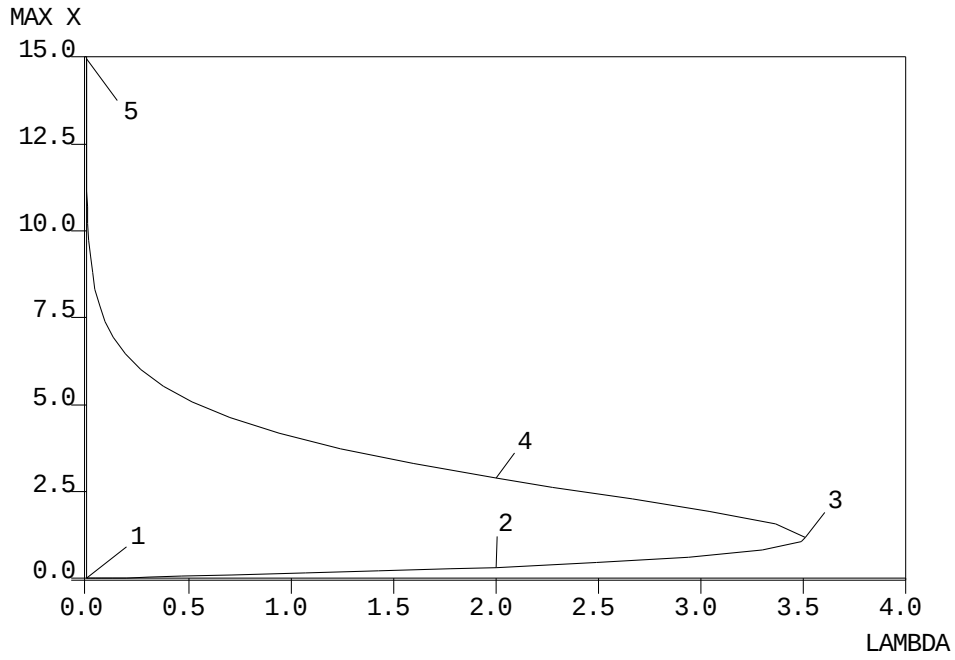

Figure 6: Bifurcation diagram for Bratu's equation.

7 Keller's Pseudo-Arclength Continuation

This method allows continuation of a branch past folds. Suppose we have a solution (x_0, λ_0) of $G(x,\lambda) = 0$, as well as the direction vector of the solution branch $(\dot{x}_0, \dot{\lambda}_0)$. Pseudo-arclength continuation consists of solving the following equations for (x_1, λ_1) :

$$G(x_1, \lambda_1) = 0,$$

$$(x_1 - x_0)^* \dot{x}_0 + (\lambda_1 - \lambda_0)\dot{\lambda}_0 - \Delta s = 0.$$

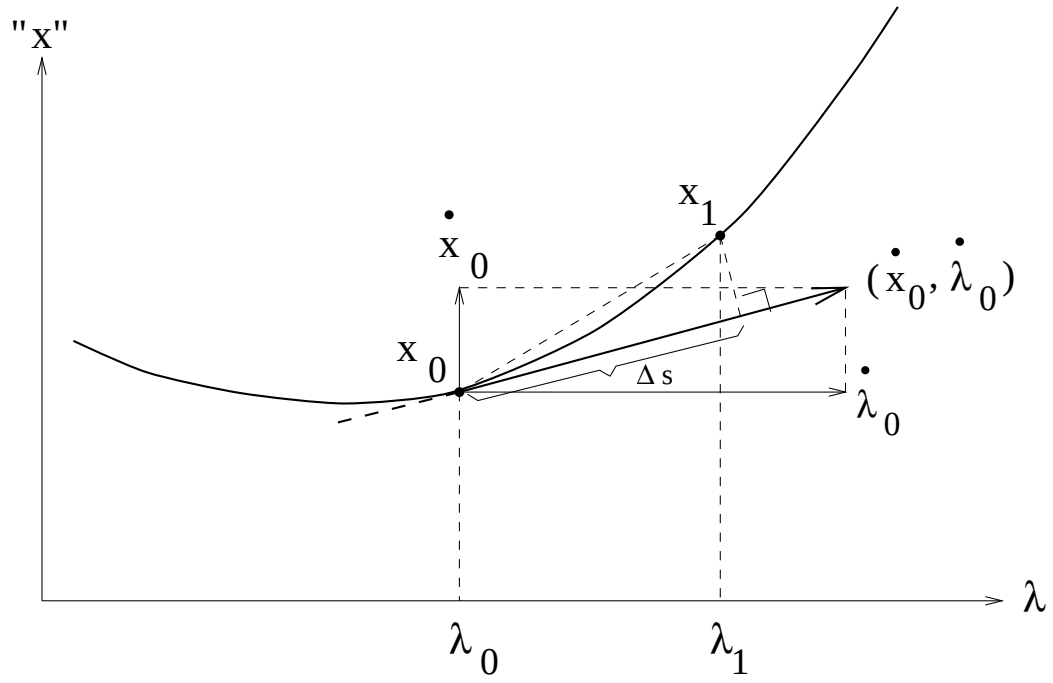

Figure 7: Graphical interpretation of pseudo-arclength continuation.

To solve these equations we use Newton's method :

$$\begin{pmatrix} (G_x^1)^{(\nu)} & (G_\lambda^1)^{(\nu)} \\ \dot{x}_0^* & \dot{\lambda}_0 \end{pmatrix} \begin{pmatrix} \Delta x_1^{(\nu)} \\ \Delta \lambda_1^{(\nu)} \end{pmatrix} = - \begin{pmatrix} G(x_1^{(\nu)}, \lambda_1^{(\nu)}) \\ (x_1^{(\nu)} - x_0)^* \dot{x}_0 - (\lambda_1^{(\nu)} - \lambda_0)\dot{\lambda}_0 \; - \; \Delta s \end{pmatrix}.$$

The next direction vector can be computed from

$$\begin{pmatrix} G_x^1 & G_\lambda^1 \\ \dot{x}_0^* & \dot{\lambda}_0 \end{pmatrix} \begin{pmatrix} \dot{x}_1 \\ \dot{\lambda}_1 \end{pmatrix} = \begin{pmatrix} 0 \\ 1 \end{pmatrix}.$$

(In practice, this direction vector is rescaled, so that it has length 1.)

EXAMPLE. Use pseudo-arclength continuation for the discretized Bratu problem. Then the matrix in Newton's method is bordered-tridiagonal as illustrated below. Such systems can be solved efficiently.

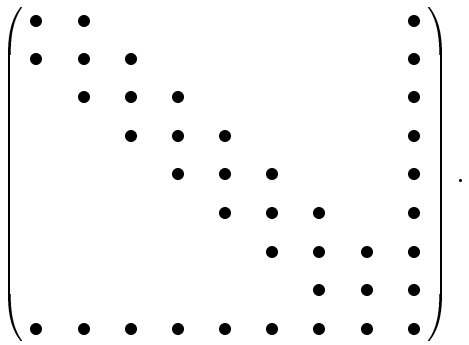

8 Formulation without Distinguished Parameter

$$F(X) = 0, \qquad F \ : \ \mathbf{R}^{n+1} \ \rightarrow \ \mathbf{R}^n$$

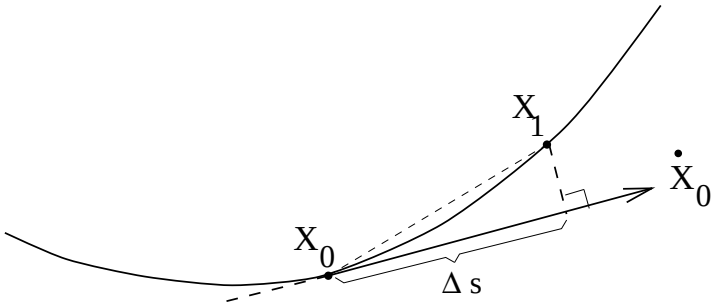

Figure 8: Pseudo-arclength continuation.

$$\text{Solve} \quad \begin{cases} F(X_1) & = 0, \\ (X_1 - X_0)^* \dot{X}_0 & = \Delta s. \end{cases}$$

9 Following Folds

To continue a fold in two parameters one can use the *extended system*

$$\boxed{\begin{array}{l} G(x, \lambda, \mu) = 0, \\ \\ G_x(x, \lambda, \mu)\phi = 0, \\ \\ \phi^* \hat{\phi} - 1 = 0. \end{array}}$$

Here $\mu \in \mathbf{R}$ is a second parameter in the equations.

The vector ϕ_0 belongs to a "reference solution" $(\hat{x}, \hat{\phi}, \hat{\lambda}, \hat{\mu})$. In practice this is latest computed solution point on the branch.

The above system has the form

$$F(X) = 0, \qquad \text{where} \quad X \equiv (x, \phi, \lambda, \mu), \qquad F \ : \ \mathbf{R}^{2n+2} \rightarrow \mathbf{R}^{2n+1}.$$

10 Branch Points

Let $G \ : \ \mathbf{R}^{n+1} \ \rightarrow \ \mathbf{R}^n$. A solution $X_0 \equiv X(s_0)$ of $G(X) = 0$ is a *branch point* if $G_X^0 \equiv G_X(X_0)$ has rank $n-1$. Suppose we have a solution branch $X(s)$ of $G(X) = 0$, where s is some parametrization.

Let $X_0 \equiv (x_0, \lambda_0)$ be a branch point. Then we must have

$$\mathcal{N}(G_X^0) = \text{Span}\{\phi_1, \phi_2\}, \qquad \mathcal{N}(G_X^{0^*}) = \text{Span}\{\psi\}.$$

We also have

$$\begin{aligned} &G(X(s)) = 0, && G^0 = G(X_0) = 0, \\ &G_X(X(s))\dot{X}(s) = 0, && G_X^0 \dot{X}_0 = 0, \\ &G_{XX}(X(s))\dot{X}(s)\dot{X}(s) + G_X(X(s))\ddot{X}(s) = 0, && G_{XX}^0 \dot{X}_0 \dot{X}_0 + G_X^0 \ddot{X}_0 = 0. \end{aligned}$$

Thus $\dot{X}_0 = \alpha\phi_1 + \beta\phi_2$, for some $\alpha, \beta \in \mathbf{R}$, and

$$\psi^* G_{XX}^0 (\alpha\phi_1 + \beta\phi_2)(\alpha\phi_1 + \beta\phi_2) + \underbrace{\psi^* G_X^0}_{=0} \ddot{X}_0 = 0,$$

$$\boxed{\underbrace{(\psi^* G_{XX}^0 \phi_1 \phi_1)}_{c_{11}} \alpha^2 + 2 \underbrace{(\psi^* G_{XX}^0 \phi_1 \phi_2)}_{c_{12}} \alpha\beta + \underbrace{(\psi^* G_{XX}^0 \phi_2 \phi_2)}_{c_{22}} \beta^2 = 0.}$$

This is the Algebraic bifurcation equation (ABE).

We want solution pairs (α, β) of the ABE with not both α and β equal to zero. If the *discriminant*

$$\Delta \equiv c_{12}^2 - c_{11} c_{22} \ > \ 0,$$

then the ABE has two distinct real nontrivial solution pairs (α_1, β_1) and (α_2, β_2), which are unique up to scaling. In such case we have a *bifurcation*, (or *branch point*) i.e., two distinct branches pass through X_0.

11 Switching branches

The first solution X_1 on the bifurcating branch can be computed from :

$$\begin{aligned} G(X_1) &= 0, \\ (X_1 - X_0)^* X_0' - \Delta s &= 0, \end{aligned} \tag{1}$$

where

$$X_0' \text{ is the direction of the bifurcating branch,}$$

with initial approximation

$$X_1^{(0)} = X_0 + \Delta s \ X_0'.$$

From the preceding discussion we see that computation of X_0' requires evaluation of G_{XX}^0.

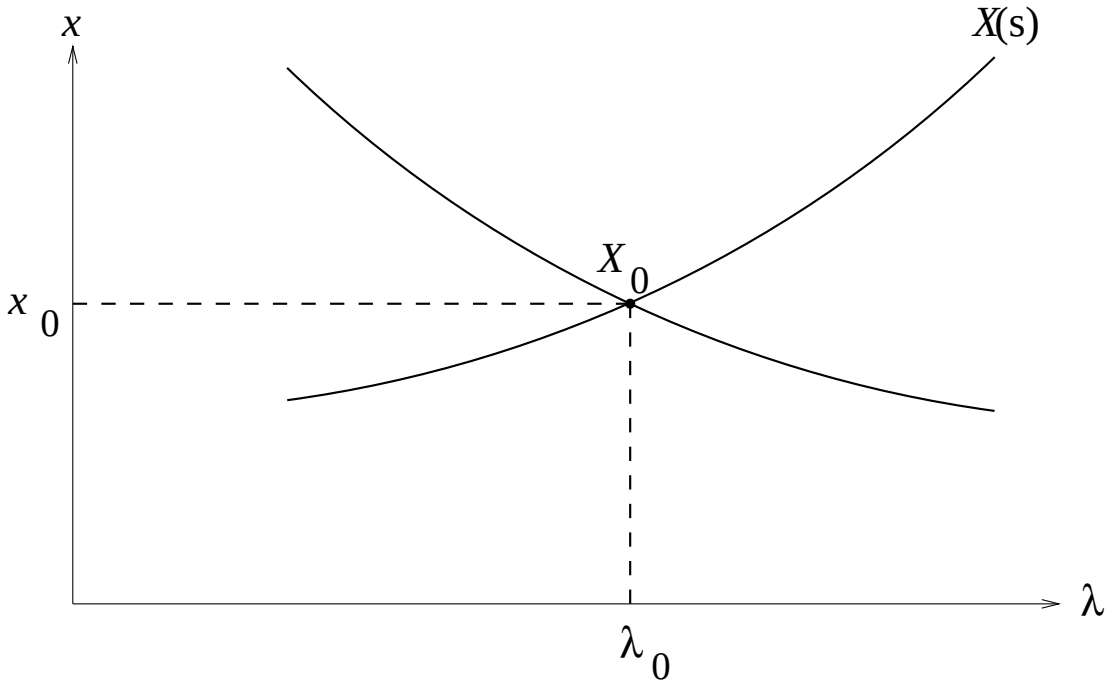

Figure 9: A solution branch $X(s) = (x(s), \lambda(s))$ of $G(x, \lambda) = 0$ with a branch point X_0.

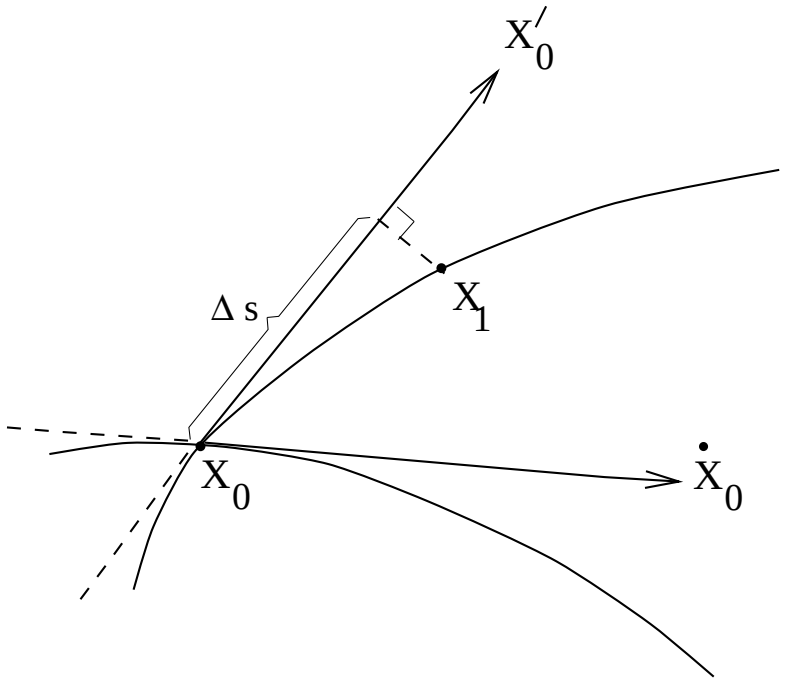

Figure 10: Switching branches using the correct bifurcation direction.

12 Simplified Branch Switching

Instead of solving Equations (1) for taking the first step on the bifurcating branch, solve :

$$G(X_1) = 0,$$

$$(X_1 - X_0)^* \phi_2 - \Delta s = 0.$$

where ϕ_2 is the second null vector of G_X^0 with

$$\phi_2 \perp \phi_1, \qquad (\phi_1 = \dot{X}_0).$$

This branch switching method works very well in most applications. Its advantage is that it does not require second derivatives.

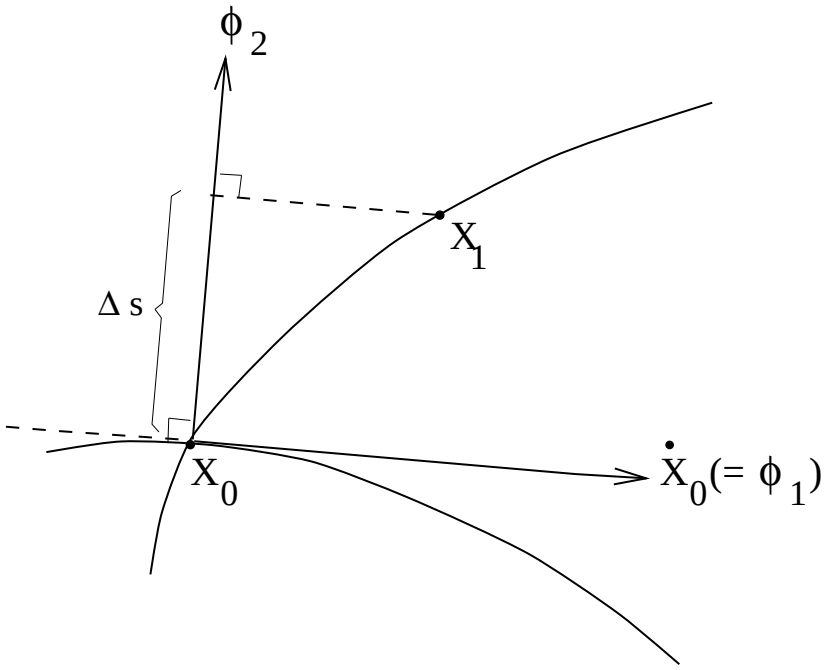

Figure 11: Switching branches using the orthogonal direction.

13 Example : The Predator-Prey Model Again

In the 2-species predator-prey model of Section 3 we have

$$G_X = (G_{x_1}\ G_{x_2}\ G_\lambda) = \begin{pmatrix} 3 - 6x_1 - x_2 - 5\lambda e^{-5x_1} & -x_1 & -(1 - e^{-5x_1}) \\ 3x_2 & -1 + 3x_1 & 0 \end{pmatrix}.$$

At the branch point

$$x_1 = x_2 = 0, \quad \lambda = 3/5,$$

we have

$$X_0 = (0, 0, 3/5),$$

and

$$G_X^0 = \begin{pmatrix} 0 & 0 & 0 \\ 0 & -1 & 0 \end{pmatrix},$$

$$\mathcal{N}(G_X^0) = \text{Span}\left\{ \begin{pmatrix} 0 \\ 0 \\ 1 \end{pmatrix}, \begin{pmatrix} 1 \\ 0 \\ 0 \end{pmatrix} \right\}, \qquad \mathcal{N}(G_X^{0^*}) = \text{Span}\left\{ \begin{pmatrix} 1 \\ 0 \end{pmatrix} \right\},$$

$$G_{XX} = \begin{pmatrix} (-6+25\lambda e^{-5x_1}, -1, -5e^{-5x_1}) & (-1,0,0) & (-5e^{-5x_1},0,0) \\ (0,3,0) & (3,0,0) & (0,0,0) \end{pmatrix},$$

$$G^0_{XX} = \begin{pmatrix} (9,-1,-5) & (-1,0,0) & (-5,0,0) \\ (0,3,0) & (3,0,0) & (0,0,0) \end{pmatrix}.$$

Thus

$$\psi^* G^0_{XX}\phi_1\phi_1 = \psi^* \begin{pmatrix} -5 & 0 & 0 \\ 0 & 0 & 0 \end{pmatrix} \phi_1 = \psi^* \begin{pmatrix} 0 \\ 0 \end{pmatrix} = 0,$$

$$\psi^* G^0_{XX}\phi_1\phi_2 = \psi^* \begin{pmatrix} -5 & 0 & 0 \\ 0 & 0 & 0 \end{pmatrix} \phi_2 = \psi^* \begin{pmatrix} -5 \\ 0 \end{pmatrix} = -5,$$

$$\psi^* G^0_{XX}\phi_2\phi_2 = \psi^* \begin{pmatrix} 9 & -1 & -5 \\ 0 & 3 & 0 \end{pmatrix} \phi_2 = \psi^* \begin{pmatrix} 9 \\ 0 \end{pmatrix} = 9.$$

Therefore the ABE is

$$-10\alpha\beta \ + \ 9\beta^2 \ = \ 0.$$

The ABE has two linearly independent solutions, namely,

$$\begin{pmatrix} \alpha \\ \beta \end{pmatrix} \ = \ \begin{pmatrix} 1 \\ 0 \end{pmatrix}, \ \begin{pmatrix} 9 \\ 10 \end{pmatrix}.$$

Thus the (non-normalized) directions of the two bifurcation branches at X_0 are

$$\dot{X}_0 = (1)\phi_1 + (0)\phi_2 = \begin{pmatrix} 0 \\ 0 \\ 1 \end{pmatrix} = \begin{pmatrix} \dot{u}_1 \\ \dot{u}_2 \\ \dot{\lambda} \end{pmatrix},$$

and

$$\dot{X}_0 = (9)\phi_1 + (10)\phi_2 = \begin{pmatrix} 10 \\ 0 \\ 9 \end{pmatrix} = \begin{pmatrix} \dot{u}_1 \\ \dot{u}_2 \\ \dot{\lambda} \end{pmatrix}.$$

14 The Hopf Bifurcation Theorem

Let $x(\lambda)$ denote a solution branch (parametrized by λ) of $f(x,\lambda) = 0$.

Suppose that a complex conjugate pair of eigenvalues

$$\alpha(\lambda) \ \pm \ i\beta(\lambda),$$

of $f_x(x(\lambda),\lambda)$ crosses the imaginary axis transversally, i.e., for some λ_0 we have

$$\alpha(\lambda_0) = 0, \qquad \beta(\lambda_0) \neq 0, \quad \text{and} \quad \dot{\alpha}(\lambda_0) \neq 0.$$

Also assume that there are no other eigenvalues on the imaginary axis. Then there is a *Hopf bifurcation* from the stationary solution branch $(x(\lambda),\lambda)$ of

$$x' = f(x,\lambda),$$

i.e., a branch of periodic solutions bifurcates from the stationary solution at (x_0,λ_0).

15 Following Hopf Bifurcations

An *extended system* for following Hopf bifurcations in two parameters is

$$F(x,\phi,\beta,\lambda;\mu) \equiv \begin{cases} f(x,\lambda,\mu)=0, \\ f_x(x,\lambda,\mu)\phi - i\beta\phi = 0, \\ \phi^*\hat{\phi} - 1 = 0, \end{cases}$$

$$F \quad : \quad \mathbf{R}^n \times \mathbf{C}^n \times \mathbf{R} \times \mathbf{R} \times \mathbf{R} \quad \rightarrow \quad \mathbf{R}^n \times \mathbf{C}^n \times \mathbf{C},$$

or, in real form,

$$F \quad : \quad \mathbf{R}^{3n+3} \quad \rightarrow \quad \mathbf{R}^{3n+2},$$

to which we want to compute a solution branch

$$(x,\phi,\beta,\lambda,\mu), \qquad \text{where} \quad x \in \mathbf{R}^n, \quad \phi \in \mathbf{C}^n, \quad \beta,\lambda,\mu \in \mathbf{R}.$$

Above, $\hat{\phi}$ belongs to a "reference solution"

$$(\hat{x},\hat{\phi},\hat{\beta},\hat{\lambda},\hat{\mu}),$$

which is typically taken to be the last computed solution point on a branch.

16 Computation of Periodic Solutions

To compute a periodic solution of period T of

$$x'(t) = f(x(t),\lambda), \qquad x(\cdot), f(\cdot) \in \mathbf{R}^n, \qquad \lambda \in \mathbf{R}\ ,$$

we first fix the interval of periodicity by the transformation $t \rightarrow \frac{t}{T}$. Then the equation becomes

$$\boxed{x'(t) = T f(x(t),\lambda)}\ , \qquad x(\cdot), f(\cdot) \in \mathbf{R}^n, \qquad T,\lambda \in \mathbf{R}. \tag{2}$$

and we seek solutions of period 1, i.e.,

$$\boxed{x(0) = x(1)}\ . \tag{3}$$

Note that the period T is one of the unknowns.

Assume that we have computed $(\hat{x}(\cdot),\hat{T},\hat{\lambda})$ and we want to compute

$$(x(\cdot),T,\lambda).$$

Equations (2) and (3) do not uniquely specify u and T, since $x(t)$ can be translated freely in time, i.e., if $x(t)$ is a periodic solution then so is $x(t+\sigma)$, for any σ.

Thus, a "*phase condition*" is needed. An example is the Poincaré phase condition

$$(x(0) - \hat{x}(0))^*\ \hat{x}^{'}(0) = 0.$$

However, below we derive a numerically more suitable phase condition.

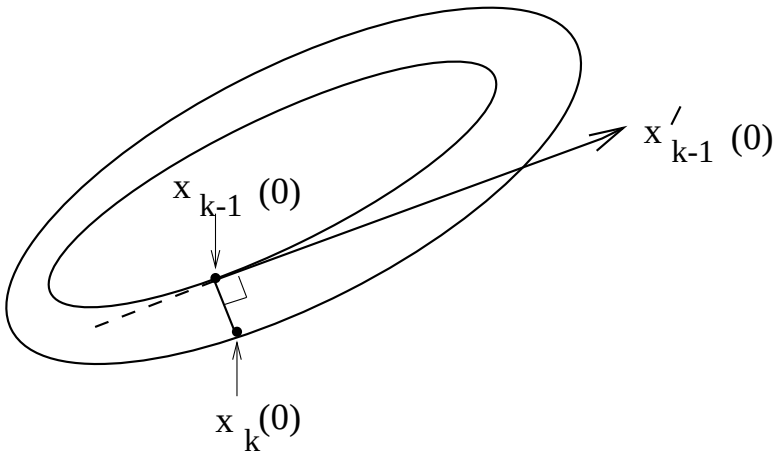

Figure 12: Graphical interpretation of the Poincaré phase condition.

17 Integral Phase Condition

If $\tilde{x}(t)$ is a solution then so is $\tilde{x}(t+\sigma)$, for any σ. It is reasonable to choose the solution that minimizes

$$D(\sigma) \equiv \int_0^1 \parallel \tilde{x}(\tau+\sigma) - \hat{x}(\tau) \parallel_2^2 \; d\tau.$$

The optimal solution $\tilde{x}(t+\sigma)$ satisfies the necessary condition $D'(\sigma) = 0$, i.e.,

$$\int_0^1 (\tilde{x}(\tau+\sigma) - \hat{x}(\tau))^* \; \tilde{x}'(\tau+\sigma) \; d\tau = 0.$$

Writing $x(t) \equiv \tilde{x}(t+\sigma)$ gives

$$\int_0^1 (x(\tau) - \hat{x}(\tau))^* \; x'(\tau) \; d\tau = 0.$$

Integration by parts, using periodicity, gives

$$\boxed{\int_0^1 x(\tau)^* \; \hat{x}'(\tau) \; d\tau = 0}\,. \tag{4}$$

18 Following Periodic Solutions

AUTO uses pseudo-arclength continuation to compute a branch of periodic solutions. This allows calculation past folds and along "vertical" branches. In this application, the pseudo-arclength equation is

$$\boxed{\int_0^1 (x(\tau) - \hat{x}(\tau))^* \dot{\hat{x}}(\tau) \; d\tau + (T - \hat{T})\dot{\hat{T}} + (\lambda - \hat{\lambda})\dot{\hat{\lambda}} = \Delta s}\,. \tag{5}$$

AUTO uses equations (2-5) for the continuation of periodic solutions.

EXERCISE. Compute and plot the periodic solutions that bifurcate from the Hopf bifurcation in

$$\begin{aligned} x_1' &= x_2, \\ x_2' &= -x_1(1-x_1) + \lambda x_2. \end{aligned}$$

(Similar to AUTO demo `phs`) This equation has a "vertical" Hopf bifurcation from the trivial solution at $\lambda = 0$. The branch terminates in a homoclinic orbit through $(x_1, x_2) = (1, 0)$. Plot some orbits versus time to see how the phase condition keeps the "peak" in almost exactly the same place. This is very advantageous for discretization methods.

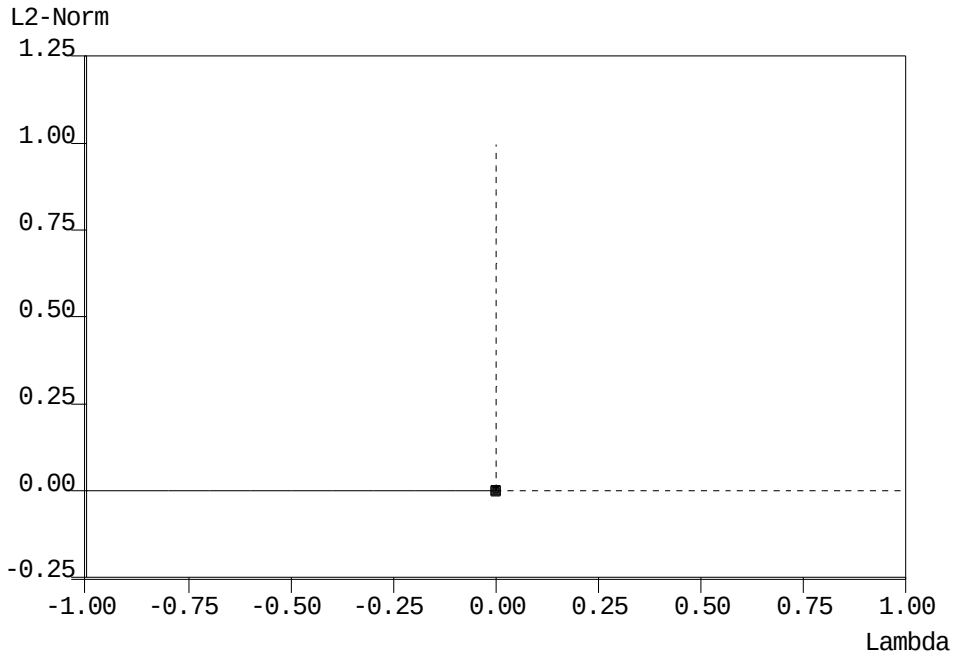

Figure 13: Bifurcation diagram for AUTO demo `phs`.

19 Computation of Homoclinic Orbits

AUTO has advanced algorithms for computing homoclinic and heteroclinic orbits and their bifurcations. Here we only mention the simplest computational approach : When continuing a period orbit, the period T may get very large. This typically means that a homoclinic orbit is approached.

To follow an (approximate) branch of homoclinic orbits do the following : Fix the period T, and instead free a second problem parameter. Restart the computation at a periodic solution of sufficiently high period.

EXERCISE.

Compute a branch of homoclinic orbits (actually a branch of *heteroclinic cycles*) in the predator prey model. (Runs 1, 3, and 7 of AUTO demo `pp2`.) Do the same for the homoclinic orbit in the AUTO demo `ab`.

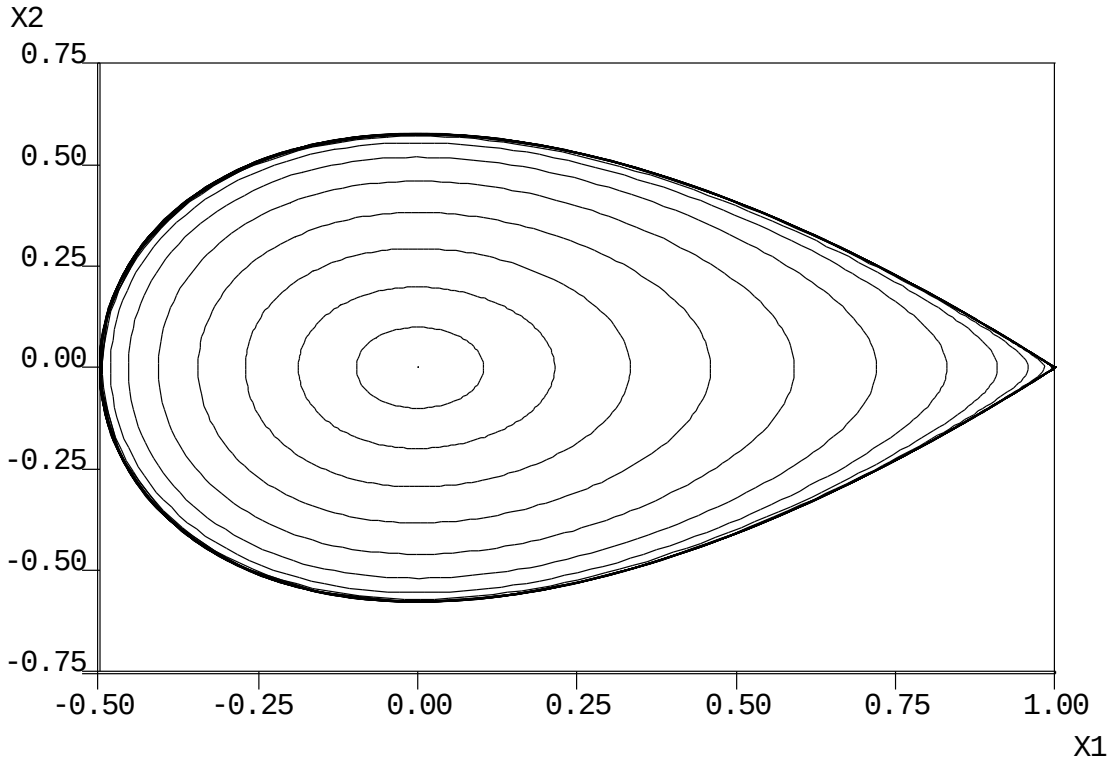

Figure 14: A phase plot of some periodic solutions.

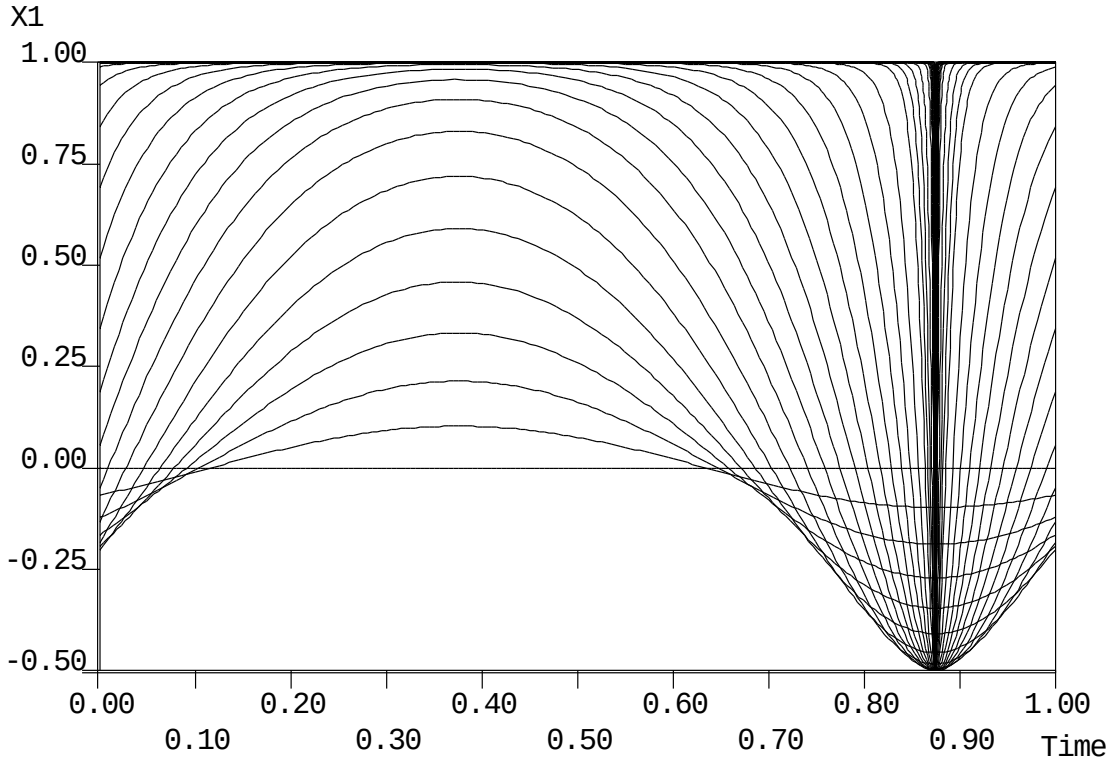

Figure 15: Solution component x_1 as a function of the scaled time variable t.

20 General ODE Boundary Value Problems

$$x'(t) = f(x(t), \lambda), \qquad t \in [0,1] \qquad x(\cdot), f(\cdot,\cdot) \in \mathbf{R}^n, \quad \lambda \in \mathbf{R}^{n_\lambda}.$$

Boundary Conditions

$$b_i(x(0), x(1), \lambda) = 0, \qquad i = 1, 2, \cdots, n_b.$$

Integral Constraints

$$\int_0^1 q_i(x(\tau), \lambda)\, d\tau = 0, \qquad i = 1, 2, \cdots, n_q.$$

Pseudo-arclength continuation

$$\int_0^1 (x(\tau) - \hat{x}(\tau))^* \dot{\hat{x}}(\tau)\, d\tau + (\lambda - \hat{\lambda})^* \dot{\hat{\lambda}} = \Delta s\ .$$

NOTE: For a solution *branch* we need $n_\lambda = n_b + n_q - n + 1$.

AUTO can do numerical continuation and branch switching for BVPs of the above form.

A specific case is the computation of stable and unstable periodic solutions, as already discussed. Another application is the computation of stable and unstable periodic solutions of integrable systems, e.g., Hamiltonian systems, as discussed below.

21 Periodic Solutions of Integrable Systems

EXAMPLE:

$$\begin{aligned} x_1' &= x_2, \\ x_2' &= -x_1(1 - x_1). \end{aligned}$$

PROBLEM: This equation has a family of periodic solutions, but no parameter!

REMEDY: Introduce a "damping parameter":

$$\begin{aligned} x_1' &= x_2, \\ x_2' &= -x_1(1 - x_1) + \lambda x_2. \end{aligned}$$

This equation has a "vertical" Hopf bifurcation from the trivial solution at $\lambda = 0$. We have already "solved" this equation!

22 Application: The Restricted 3-Body Problem.

$$\ddot{x} = 2\dot{y} + x - \mu - (1-\mu)xr^{-3} - \mu(x-1)\rho^{-3},$$

$$\ddot{y} = -2\dot{x} + y - (1-\mu)yr^{-3} - \mu y\rho^{-3},$$

where

$$r = \sqrt{x^2+y^2}, \qquad \rho = \sqrt{(x-1)^2+y^2}.$$

Above, (x, y) denotes the position of the zero-mass body. For the earth-moon system $\mu \approx 0.012$. This equation has one integral of motion, the "Jacobi-constant", given by

$$E = (x-\mu)^2 + y^2 + \frac{2(1-\mu)}{r} + \frac{2\mu}{\rho} - \dot{x}^2 - \dot{y}^2.$$

OBJECTIVE: Compute the family of planar periodic orbits that surround the Lagrange point L1 ("libration point") between the earth and the moon. These orbits are known as Lyapunov orbits.

COMPUTATIONAL FORMULATION:

$$\begin{aligned}
\dot{x} &= Tv_x + \lambda E_x, \\
\dot{y} &= Tv_y + \lambda E_y, \\
\dot{v}_x &= T[2v_y + x - \mu - (1-\mu)xr^{-3} - \mu(x-1)\rho^{-3}] + \lambda E_{v_x}, \\
\dot{v}_y &= T[-2v_x + y - (1-\mu)yr^{-3} - \mu y\rho^{-3}] + \lambda E_{v_y},
\end{aligned}$$

$$x(1) = x(0), \qquad y(1) = y(0), \qquad v_x(1) = v_x(0), \qquad v_y(1) = v_y(0).$$

The independent time-variable t has been scaled, as before. A phase condition is added, as before. T is the unknown period. The unfolding term $\lambda\nabla E$ is introduced to regularize the continuation, just like the parametrized damping term in the earlier model. λ will be "zero", once solved for.

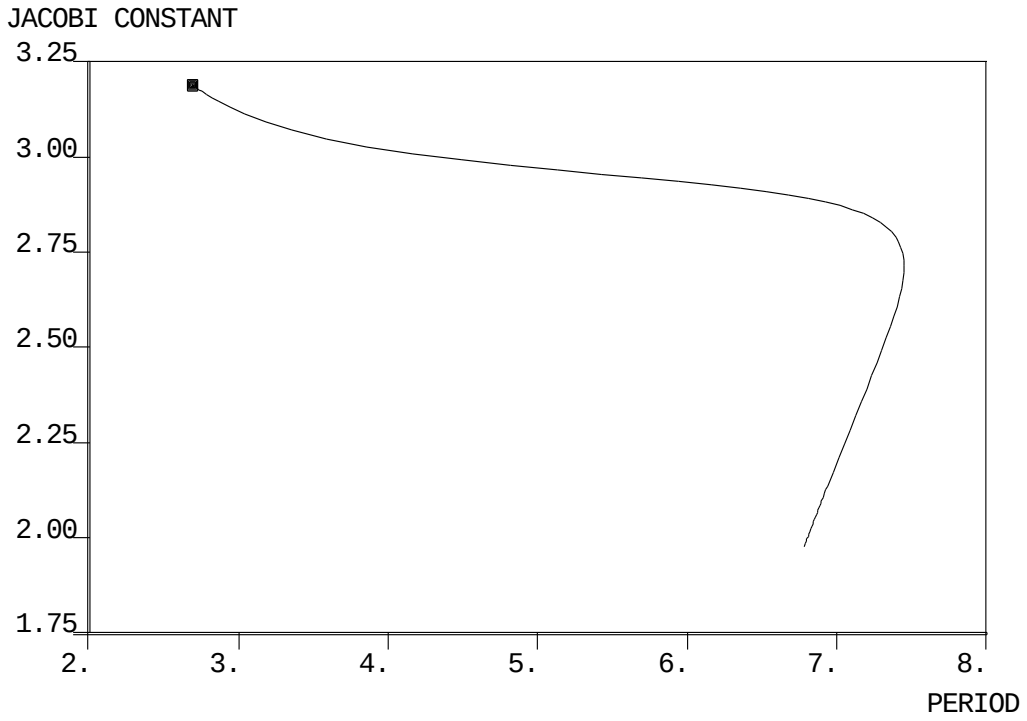

Figure 16: The branch of planar periodic orbits that bifurcates from L1.

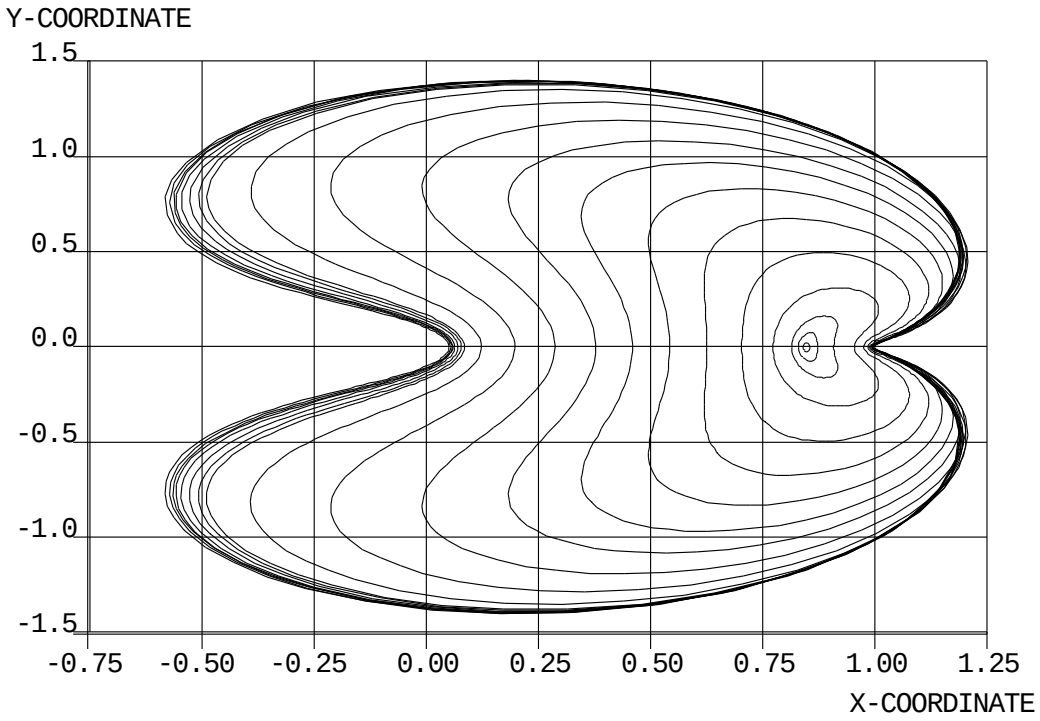

Figure 17: Some Lyapunov Orbits.

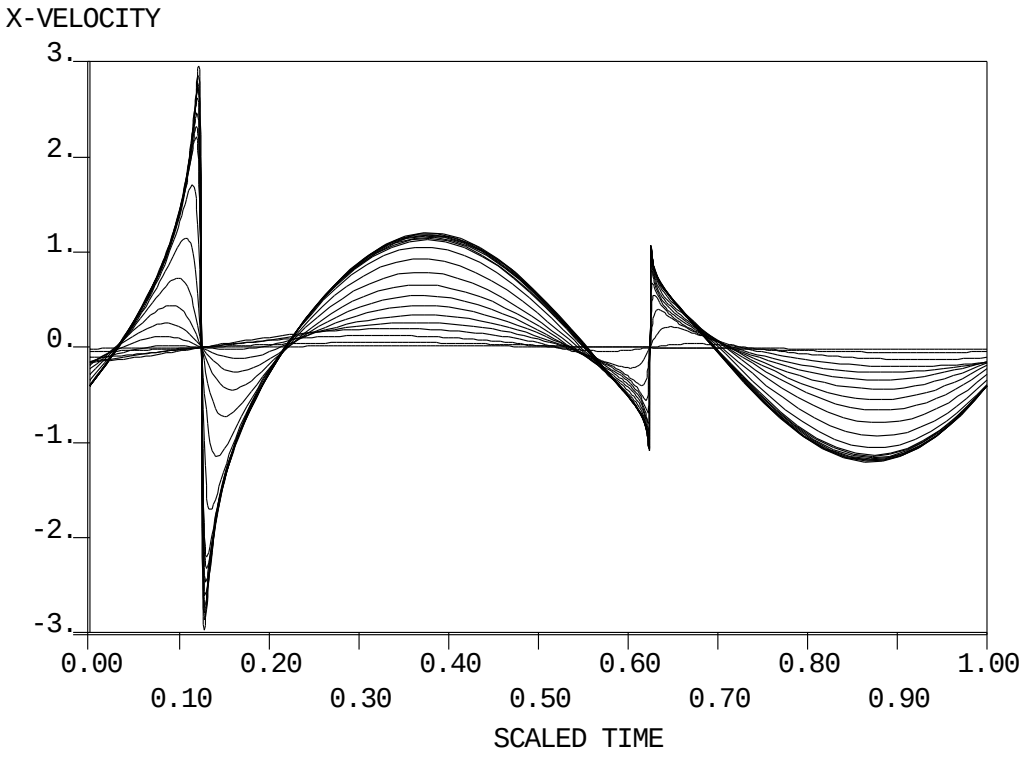

Figure 18: x-Velocity of some Lyapunov Orbits.

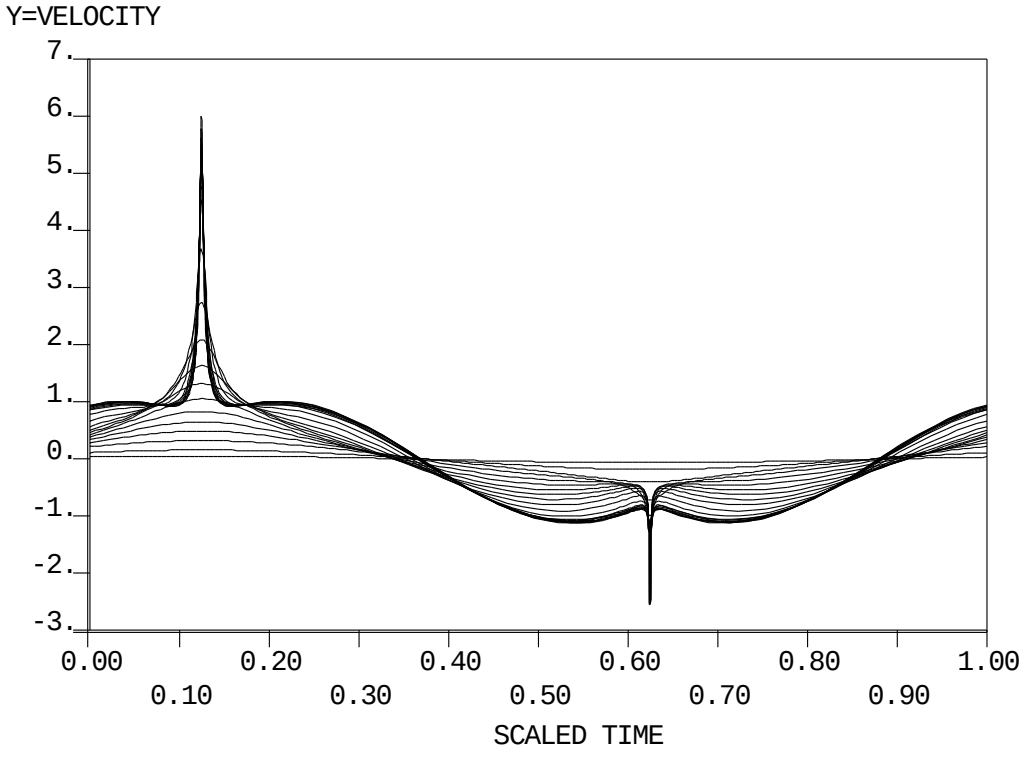

Figure 19: y-Velocity of some Lyapunov Orbits.

23 Application: The Full 3-Body Problem.

$$\ddot{\mathbf{x}}_1 = -m_2 \frac{\mathbf{x}_1 - \mathbf{x}_2}{|\mathbf{x}_1 - \mathbf{x}_2|^3} - m_3 \frac{\mathbf{x}_1 - \mathbf{x}_3}{|\mathbf{x}_1 - \mathbf{x}_3|^3} \ ,$$

$$\ddot{\mathbf{x}}_2 = -m_1 \frac{\mathbf{x}_2 - \mathbf{x}_1}{|\mathbf{x}_1 - \mathbf{x}_2|^3} - m_3 \frac{\mathbf{x}_2 - \mathbf{x}_3}{|\mathbf{x}_2 - \mathbf{x}_3|^3} \ ,$$

$$\ddot{\mathbf{x}}_3 = -m_2 \frac{\mathbf{x}_3 - \mathbf{x}_2}{|\mathbf{x}_3 - \mathbf{x}_2|^3} - m_1 \frac{\mathbf{x}_3 - \mathbf{x}_1}{|\mathbf{x}_1 - \mathbf{x}_3|^3} \ .$$

$$\mathbf{x}_i \equiv \begin{pmatrix} x_i \\ y_i \\ z_i \end{pmatrix} .$$

OBJECTIVE: Find periodic solutions.

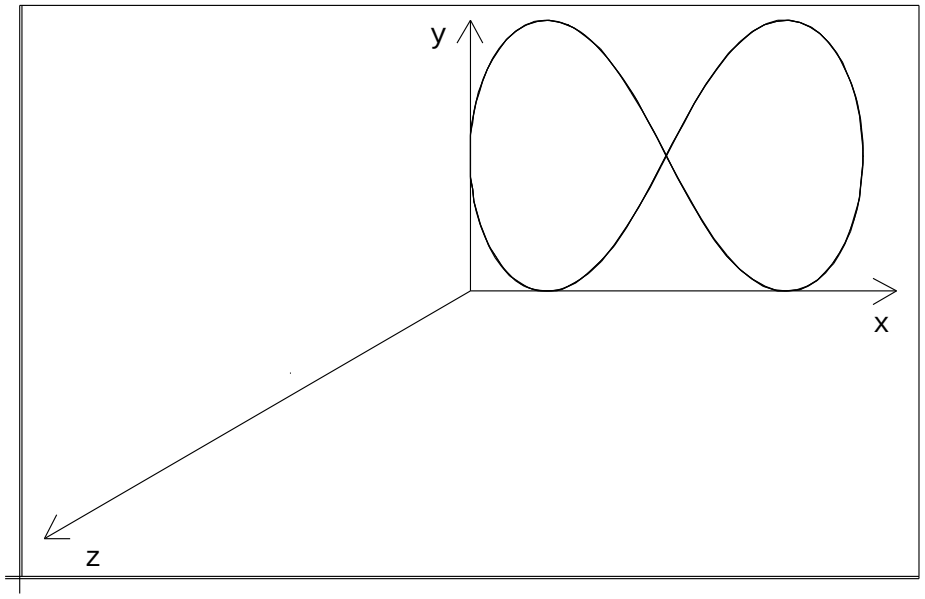

Figure 20: A Figure-8 Orbit for the 3-Body Problem; $m_1 = m_2 = m_3 = 1$. (Montgomery, Chenciner (2000), and Simo (2000).)

BASIC COMPUTATIONAL FORMULATION:

$$\dot{\mathbf{x}}_1 = T\mathbf{v}_1, \qquad \dot{\mathbf{x}}_2 = T\mathbf{v}_2, \qquad \dot{\mathbf{x}}_3 = T\mathbf{v}_3,$$

$$\dot{\mathbf{v}}_1 = -T\{m_2\frac{\mathbf{x}_1 - \mathbf{x}_2}{|\mathbf{x}_1 - \mathbf{x}_2|^3} + m_3\frac{\mathbf{x}_1 - \mathbf{x}_3}{|\mathbf{x}_1 - \mathbf{x}_3|^3}\},$$

$$\dot{\mathbf{v}}_2 = -T\{m_1\frac{\mathbf{x}_2 - \mathbf{x}_1}{|\mathbf{x}_1 - \mathbf{x}_2|^3} + m_3\frac{\mathbf{x}_2 - \mathbf{x}_3}{|\mathbf{x}_2 - \mathbf{x}_3|^3}\},$$

$$\dot{\mathbf{v}}_3 = -T\{m_2\frac{\mathbf{x}_3 - \mathbf{x}_2}{|\mathbf{x}_3 - \mathbf{x}_2|^3} + m_1\frac{\mathbf{x}_3 - \mathbf{x}_1}{|\mathbf{x}_1 - \mathbf{x}_3|^3}\},$$

$$\mathbf{x}_1(0) - \mathbf{x}_1(1) = 0, \qquad \mathbf{x}_2(0) - \mathbf{x}_2(1) = 0, \qquad \mathbf{x}_3(0) - \mathbf{x}_3(1) = 0,$$

$$\mathbf{v}_1(0) - \mathbf{v}_1(1) = 0, \qquad \mathbf{v}_2(0) - \mathbf{v}_2(1) = 0, \qquad \mathbf{v}_3(0) - \mathbf{v}_3(1) = 0,$$

where T is the unknown period.

PROBLEM: Periodic solutions are not unique, due to:

- phase-shift invariance
- Hamiltonian structure
- scaling invariance $\mathbf{x} \to c\mathbf{x}, \quad \mathbf{v} \to c^{-\frac{1}{2}}\mathbf{v}, \quad T \to c^{\frac{3}{2}}T$
- x, y, z - translations
- x, y, z - rotations

REMEDY: Add constraints:

- Phase:
$$\sum_{i=1}^{n} \int_0^1 \langle \mathbf{x}_i(\tau), \hat{\mathbf{x}}_i'(\tau) \rangle \, d\tau = 0 \ .$$

- Hamiltonian structure: Use damping parameter + pseudo-arclength continuation!

- Scaling invariance: Fix the period T.

- Translation:
$$\sum_{i=1}^{n} \int_0^1 \mathbf{x}_i(\tau) - \hat{\mathbf{x}}_i(\tau) \, d\tau = 0 \ .$$

- x-Rotation:
$$\sum_{i=1}^{n} \int_0^1 [y_i(\tau) - \hat{y}_i(\tau)] z_i(\tau) - [z_i(\tau) - \hat{z}_i(\tau)] y_i(\tau) \, d\tau = 0 \ .$$

- y-Rotation:
$$\sum_{i=1}^{n} \int_0^1 -[x_i(\tau) - \hat{x}_i(\tau)] z_i(\tau) + [z_i(\tau) - \hat{z}_i(\tau)] x_i(\tau) \, d\tau = 0 \ .$$

- z-Rotation:
$$\sum_{i=1}^{n} \int_0^1 [x_i(\tau) - \hat{x}_i(\tau)] y_i(\tau) - [y_i(\tau) - \hat{y}_i(\tau)] x_i(\tau) \, d\tau = 0 \ .$$

Derivation of the Integral that Fixes the z-Rotation:

z-Rotation:
$$\mathbf{x} \to A(\theta)\mathbf{x}$$

$$\begin{pmatrix} x \\ y \\ z \end{pmatrix} \to \begin{pmatrix} \cos\theta & \sin\theta & 0 \\ -\sin\theta & \cos\theta & 0 \\ 0 & 0 & 1 \end{pmatrix} \begin{pmatrix} x \\ y \\ z \end{pmatrix}$$

If $\tilde{\mathbf{x}}(t)$ is a solution then so is $A(\theta)\tilde{\mathbf{x}}(t)$.

Choose θ that minimizes

$$D(\theta) \equiv \int_0^1 |A(\theta)\tilde{\mathbf{x}}(\tau) - \hat{\mathbf{x}}(\tau)|^2 d\tau.$$

This gives

$$\int_0^1 \langle A(\theta)\tilde{\mathbf{x}}(\tau) - \hat{\mathbf{x}}(\tau), \dot{A}(\theta)\tilde{\mathbf{x}}(\tau)\rangle \; d\tau = 0,$$

i.e.,

$$\int_0^1 \tilde{\mathbf{x}}^*(\tau)A^*(\theta)\dot{A}(\theta)\tilde{\mathbf{x}}(\tau) - \hat{\mathbf{x}}^*(\tau)\dot{A}(\theta)\tilde{\mathbf{x}}(\tau) \; d\tau = 0.$$

The optimal solution is $\mathbf{x}(t) \equiv A(\theta)\tilde{\mathbf{x}}(t)$.

We have $\tilde{\mathbf{x}}(t) = A^{-1}(\theta)\mathbf{x}(t) = A^*(\theta)\mathbf{x}(t)$.

Then

$$\int_0^1 \mathbf{x}^*(\tau)\dot{A}(\theta)A^*(\theta)\mathbf{x}(\tau) - \hat{\mathbf{x}}^*(\tau)\dot{A}(\theta)A^*(\theta)\mathbf{x}(\tau) \; d\tau = 0,$$

i.e.,

$$\int_0^1 (\mathbf{x}^*(\tau) - \hat{\mathbf{x}}^*(\tau))\dot{A}(\theta)A^*(\theta)\mathbf{x}(\tau) \; d\tau = 0.$$

Now

$$\dot{A}(\theta)A^*(\theta) = \begin{pmatrix} 0 & 1 & 0 \\ -1 & 0 & 0 \\ 0 & 0 & 1 \end{pmatrix},$$

so that the integral constraint (summed over all three bodies) becomes

$$\boxed{\sum_{i=1}^n \int_0^1 [x_i(\tau) - \hat{x}_i(\tau)]y_i(\tau) - [y_i(\tau) - \hat{y}_i(\tau)]x_i(\tau) \; d\tau = 0}\,.$$

ANOTHER PROBLEM: Too many equations! (18 ODEs with 18 periodicity conditions and 7 integral constraints)

REMEDY: Add "unfolding parameters":

FULL COMPUTATIONAL FORMULATION:

$$\dot{\mathbf{x}}_1 = T\mathbf{v}_1, \qquad \dot{\mathbf{x}}_2 = T\mathbf{v}_2, \qquad \dot{\mathbf{x}}_3 = T\mathbf{v}_3,$$

$$\dot{\mathbf{v}}_1 = -T\{m_2\frac{\mathbf{x}_1-\mathbf{x}_2}{|\mathbf{x}_1-\mathbf{x}_2|^3} + m_3\frac{\mathbf{x}_1-\mathbf{x}_3}{|\mathbf{x}_1-\mathbf{x}_3|^3}\} + \lambda_1\mathbf{v}_1 + \begin{pmatrix}\lambda_2\\ \lambda_3\\ \lambda_4\end{pmatrix} + \lambda_5\begin{pmatrix}0\\ z_1\\ -y_1\end{pmatrix} + \lambda_6\begin{pmatrix}-z_1\\ 0\\ x_1\end{pmatrix} + \lambda_7\begin{pmatrix}y_1\\ -x_1\\ 0\end{pmatrix},$$

$$\dot{\mathbf{v}}_2 = -T\{m_1\frac{\mathbf{x}_2-\mathbf{x}_1}{|\mathbf{x}_1-\mathbf{x}_2|^3} + m_3\frac{\mathbf{x}_2-\mathbf{x}_3}{|\mathbf{x}_2-\mathbf{x}_3|^3}\} + \lambda_1\mathbf{v}_2 + \begin{pmatrix}\lambda_2\\ \lambda_3\\ \lambda_4\end{pmatrix} + \lambda_5\begin{pmatrix}0\\ z_2\\ -y_2\end{pmatrix} + \lambda_6\begin{pmatrix}-z_2\\ 0\\ x_2\end{pmatrix} + \lambda_7\begin{pmatrix}y_2\\ -x_2\\ 0\end{pmatrix},$$

$$\dot{\mathbf{v}}_3 = -T\{m_2\frac{\mathbf{x}_3-\mathbf{x}_2}{|\mathbf{x}_3-\mathbf{x}_2|^3} + m_1\frac{\mathbf{x}_3-\mathbf{x}_1}{|\mathbf{x}_1-\mathbf{x}_3|^3}\} + \lambda_1\mathbf{v}_3 + \begin{pmatrix}\lambda_2\\ \lambda_3\\ \lambda_4\end{pmatrix} + \lambda_5\begin{pmatrix}0\\ z_3\\ -y_3\end{pmatrix} + \lambda_6\begin{pmatrix}-z_3\\ 0\\ x_3\end{pmatrix} + \lambda_7\begin{pmatrix}y_3\\ -x_3\\ 0\end{pmatrix},$$

where T, λ_1, λ_2, λ_3, λ_4, λ_5, λ_6, λ_7, are unknown. (The λ_i will be "zero"!)

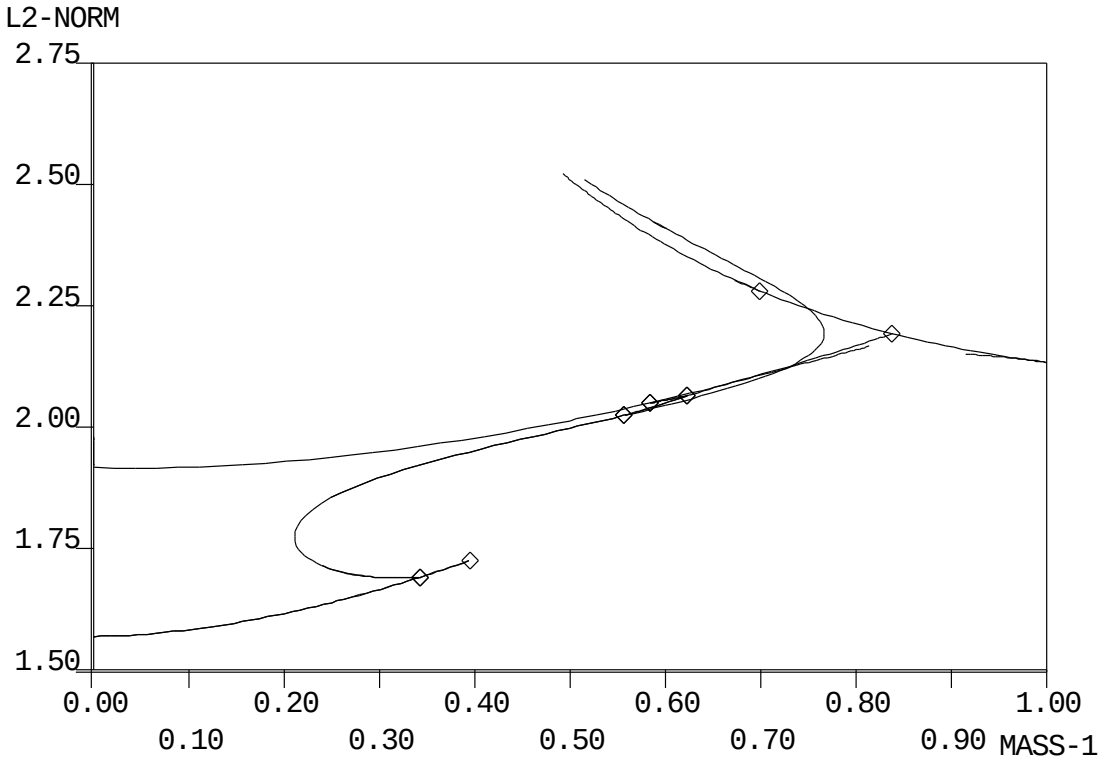

Figure 21: A Bifurcation Diagram for the 3-Body Problem.

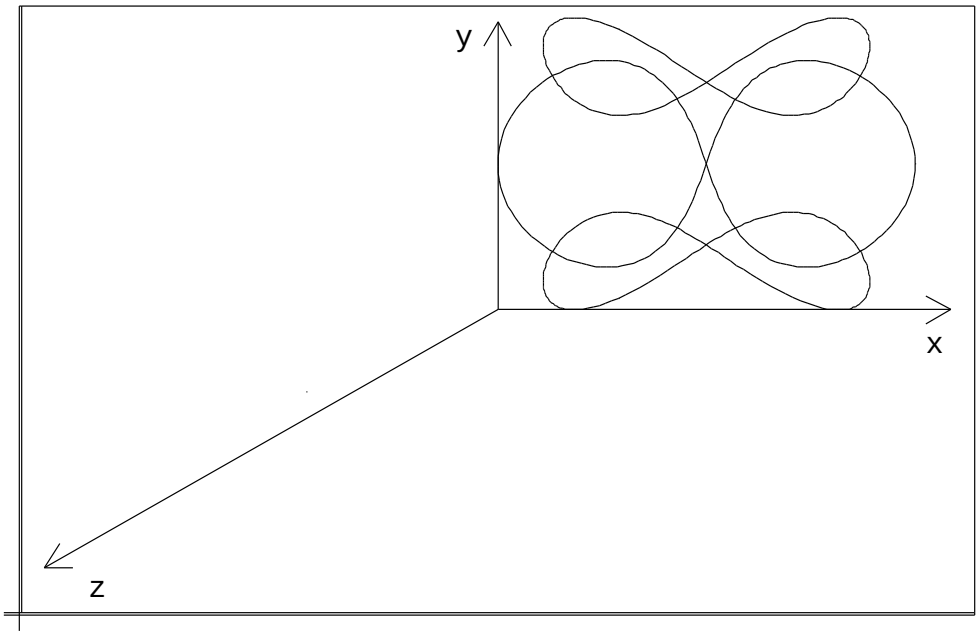

Figure 22: A Planar Periodic Orbit.

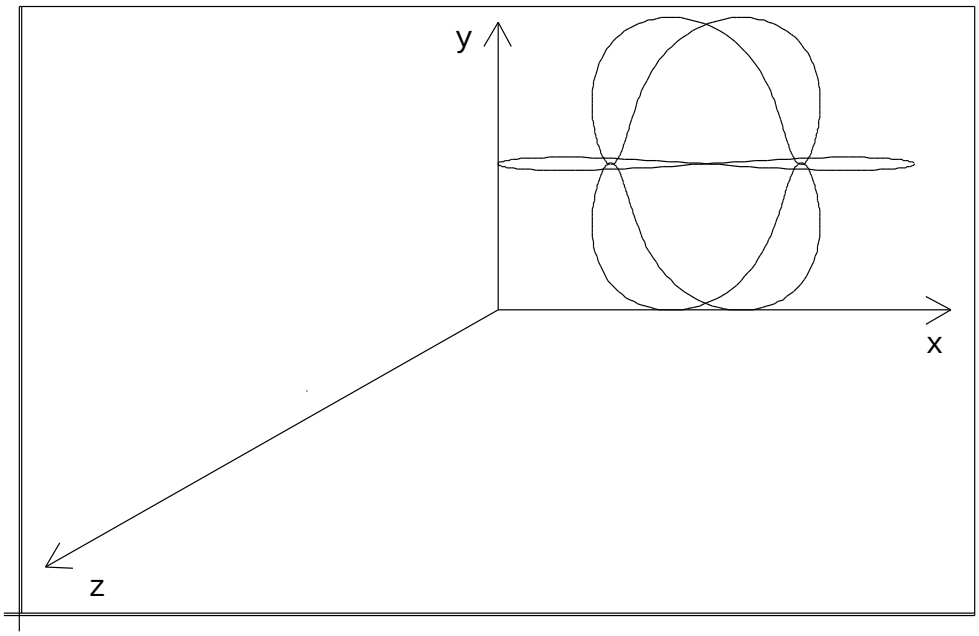

Figure 23: A Planar Periodic Orbit near Collision.

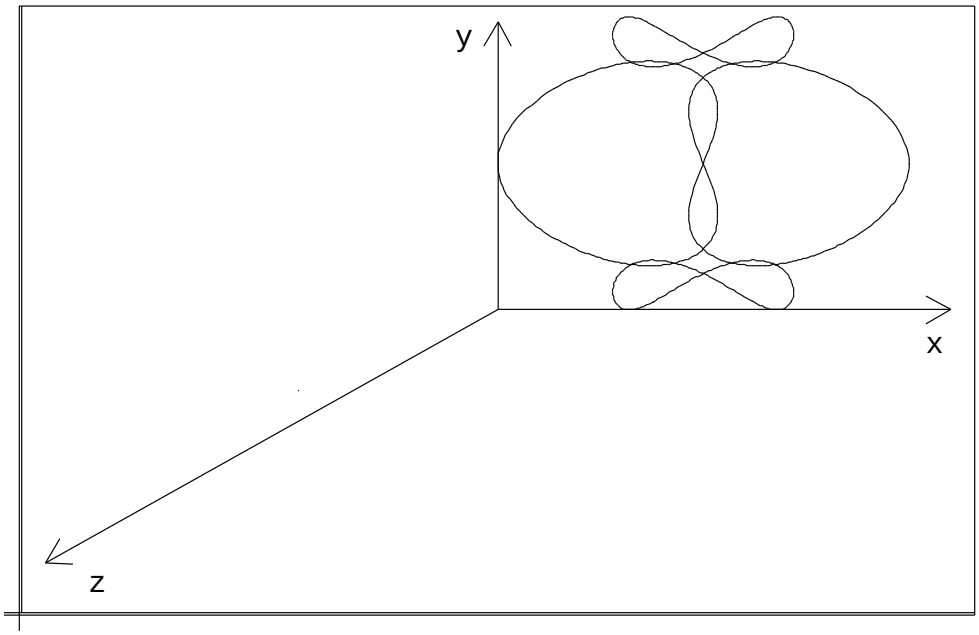

Figure 24: Another Planar Periodic Orbit near Collision.

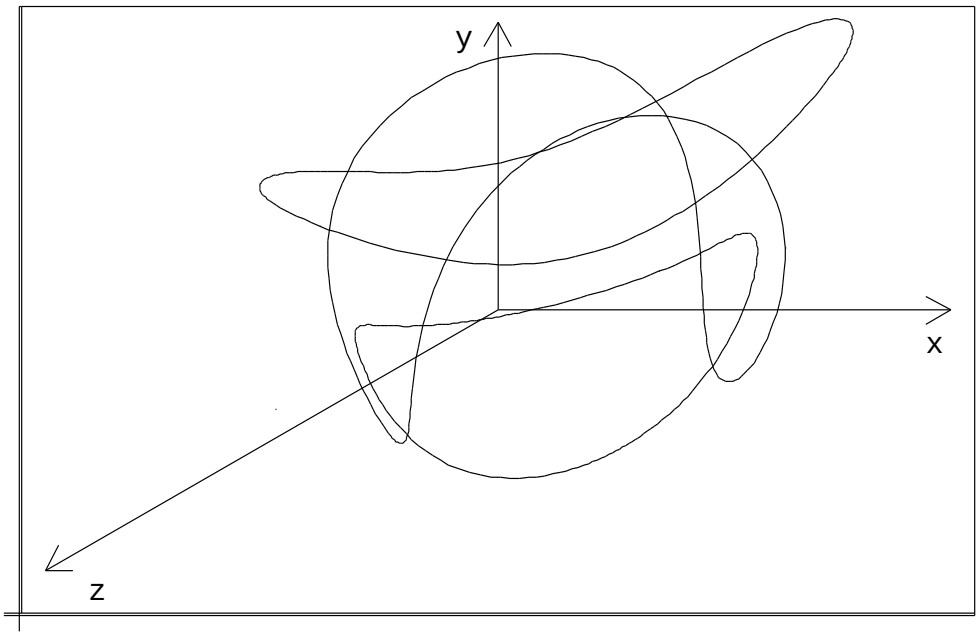

Figure 25: A Non-Planar Periodic Orbit.

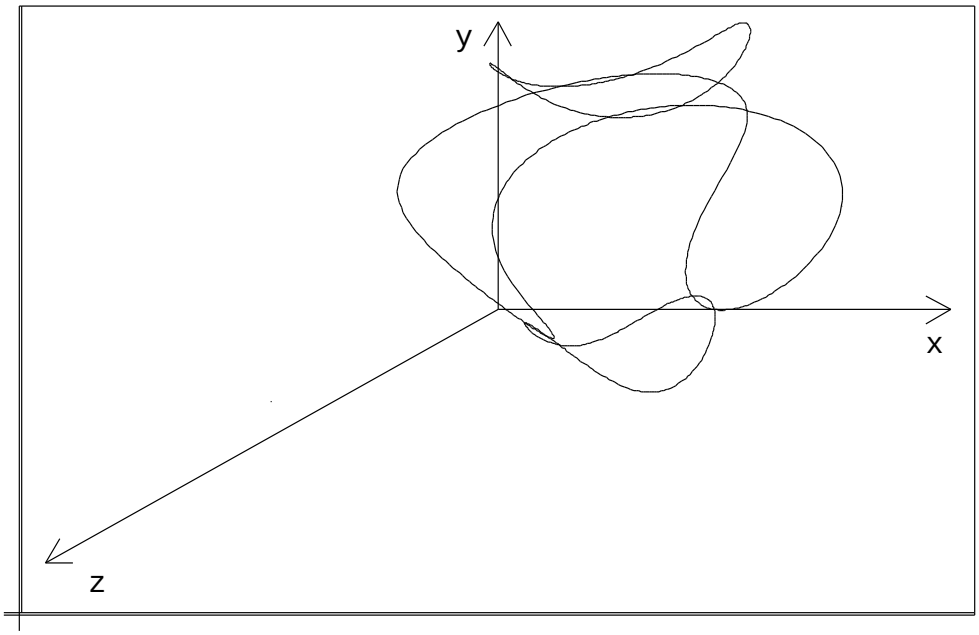

Figure 26: A Non-Planar Orbit near Collision.

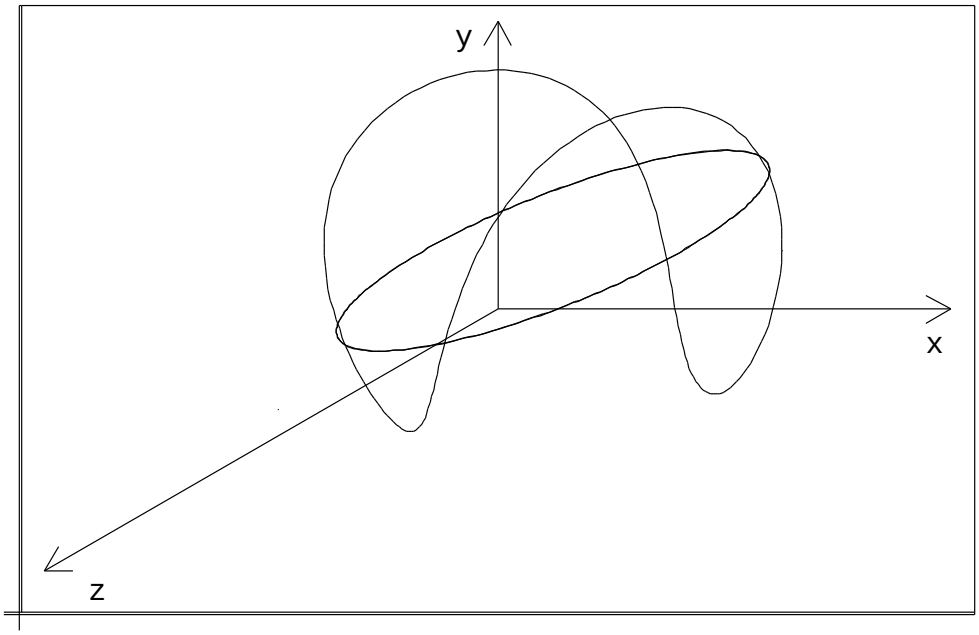

Figure 27: A Periodic Solution to the Restricted 3-Body Problem ($m_1 = 0$).

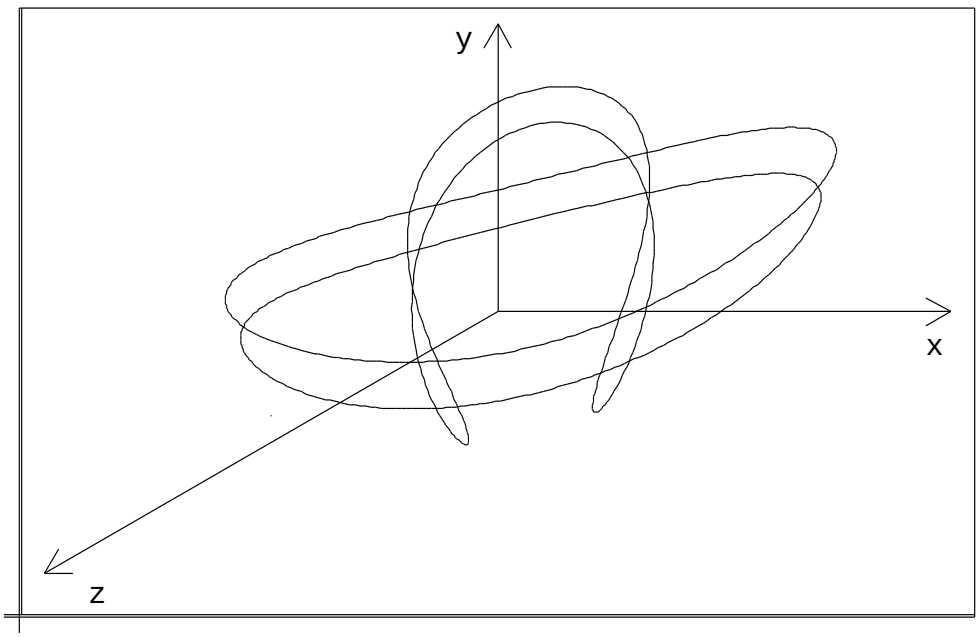

Figure 28: Another Non-Planar Periodic Orbit.

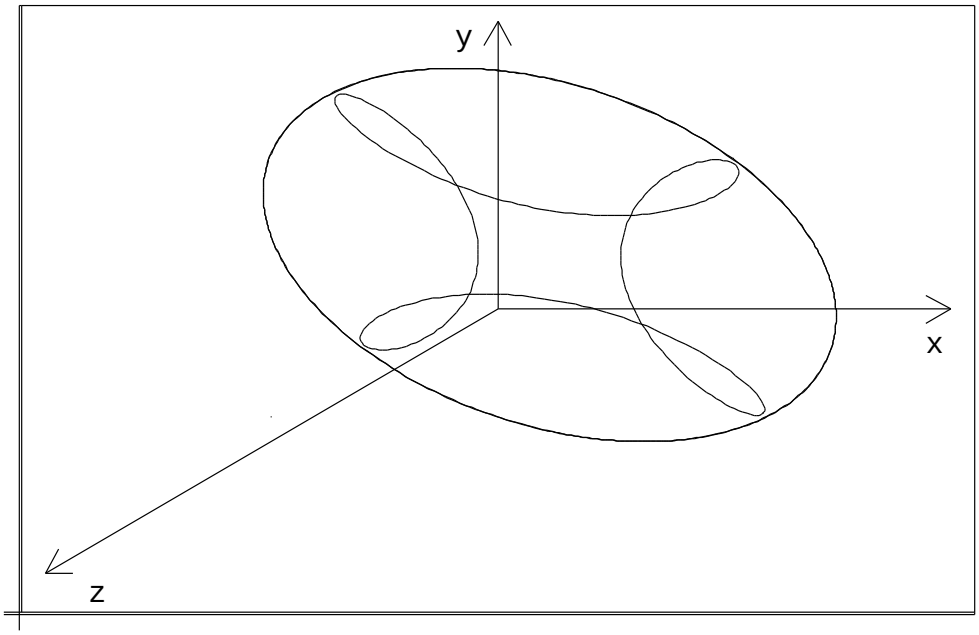

Figure 29: A Planar Solution to the Restricted 3-Body Problem ($m_1 = 0$).

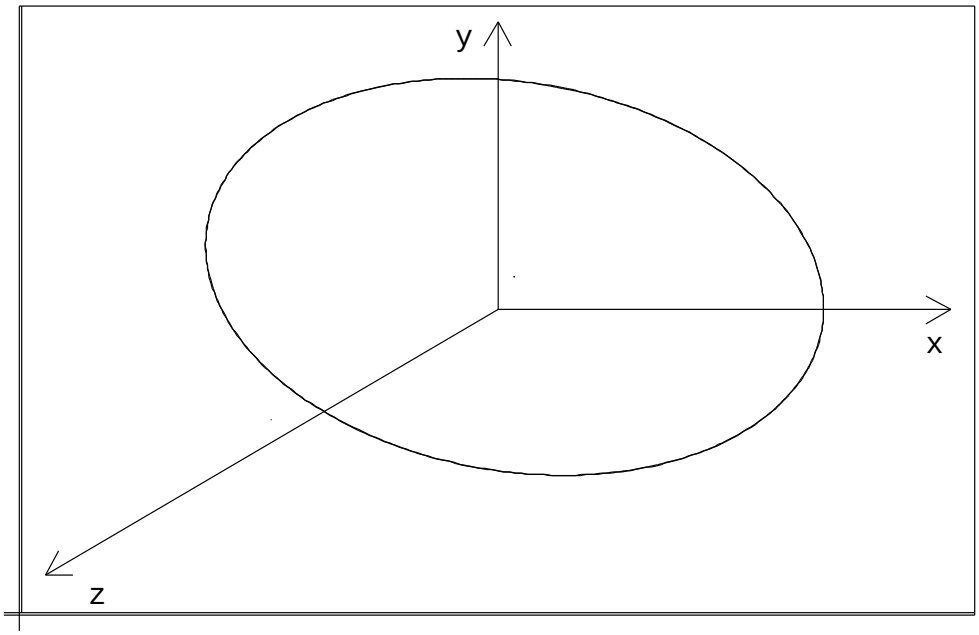

Figure 30: A (Singular) Planar Periodic Orbit.

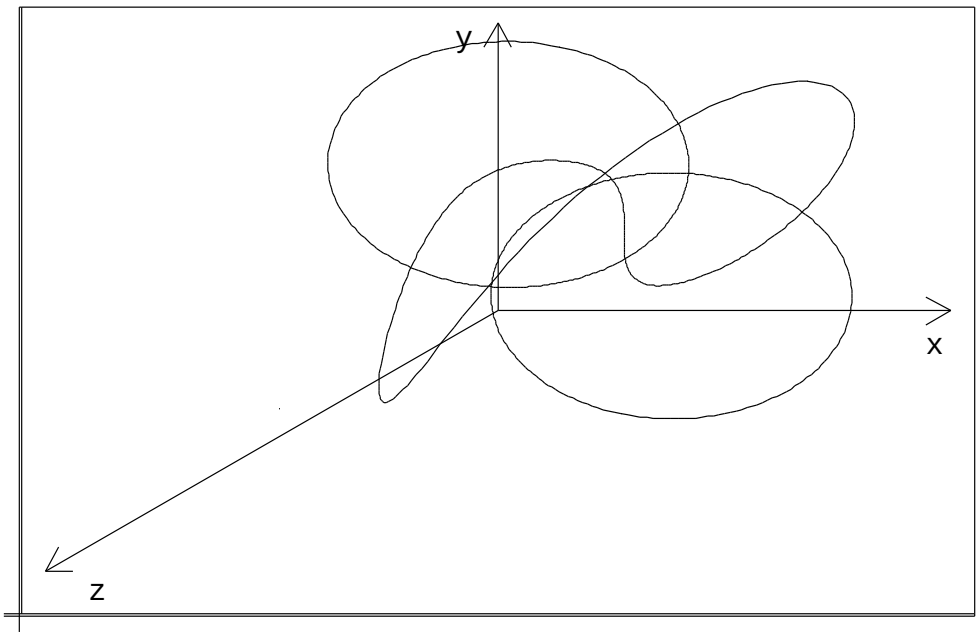

Figure 31: Body 2 and Body 3 are Planar; $m_1 = 0$.

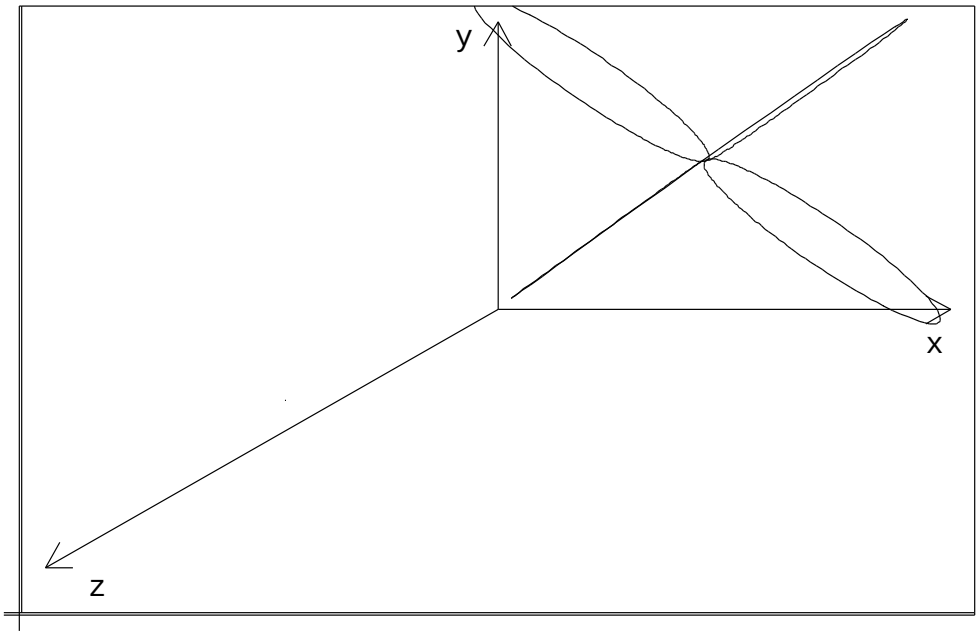

Figure 32: Near-Collision; Body 2 and Body 3 are Planar; $m_1 = 0$.

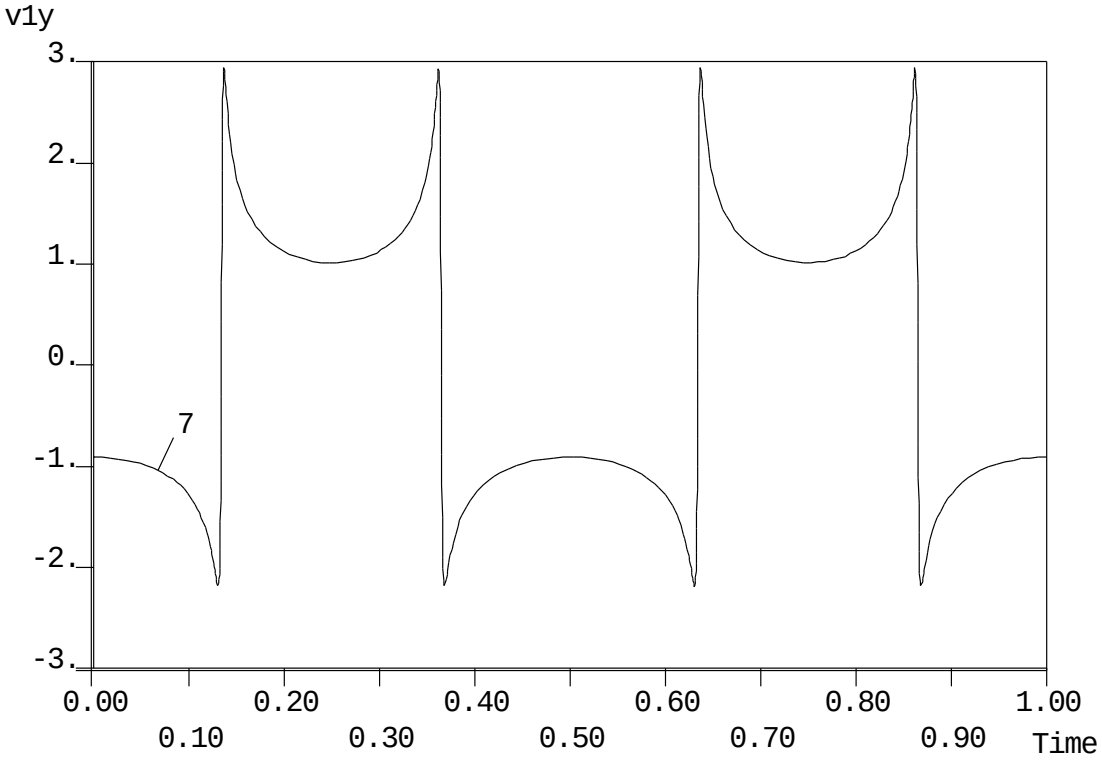

Figure 33: A y-Velocity-Profile over one Period.

24 Discretization: Orthogonal Collocation

Collocation method : Find $p \in C[0,1]$ such that

- p is a polynomial of degree m or less inside each mesh interval.
- Collocation: $p_j^{'}(z_{ji}) = f(p_j(z_{ji}), \lambda), \qquad i = 1, \cdots, m, \quad j = 1, 2, \cdots, N$
- p satisfies the boundary and integral constraints.

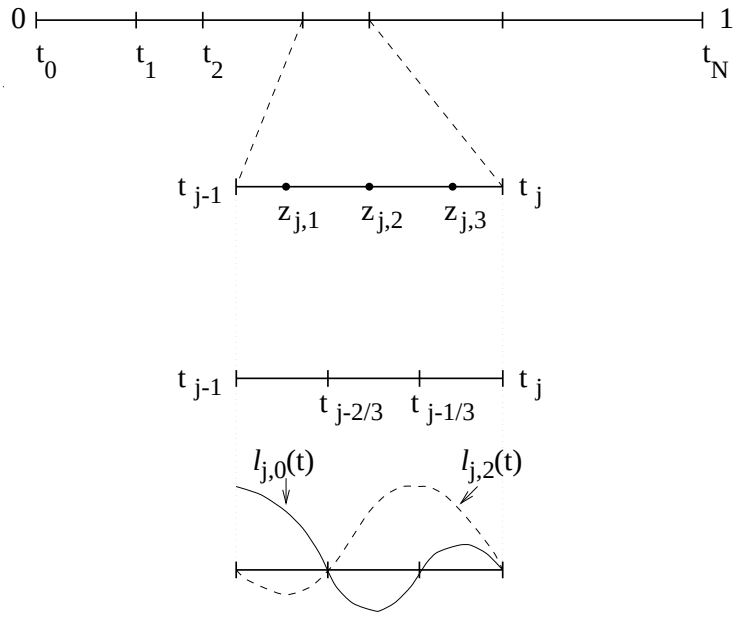

Figure 34: Mesh points, Gauss collocation points, Local basis.

ACCURACY:

$$\| p - x \|_\infty = \mathcal{O}(h^m).$$

At the main meshpoints t_j we have *superconvergence* :

$$max_j \mid p(t_j) - x(t_j) \mid = \mathcal{O}(h^{2m}).$$

The scalar variables λ are also superconvergent.

SPECIFIC IMPLEMENTATION:

Lagrange basis polynomials :

$$\{ \ell_{ji}(t) \}, \qquad j = 1, 2, \cdots, N, \qquad i = 0, 1, \cdots, m$$

Polynomial representation :

$$p_j(t) = \sum_{i=0}^{m} x_{j-1+\frac{i}{m}} \ \ell_{ji}(t).$$

COLLOCATION SOFTWARE:

- COLSYS (and successor, COLNEW) (Ascher, Christiansen, Russell)
- COLDAE (Ascher, Spiteri)
- AUTO
- CONTENT (Kuznetsov, Levitin)
- DDE-BIFTOOL (Engelborghs)

Structure of the Jacobian.

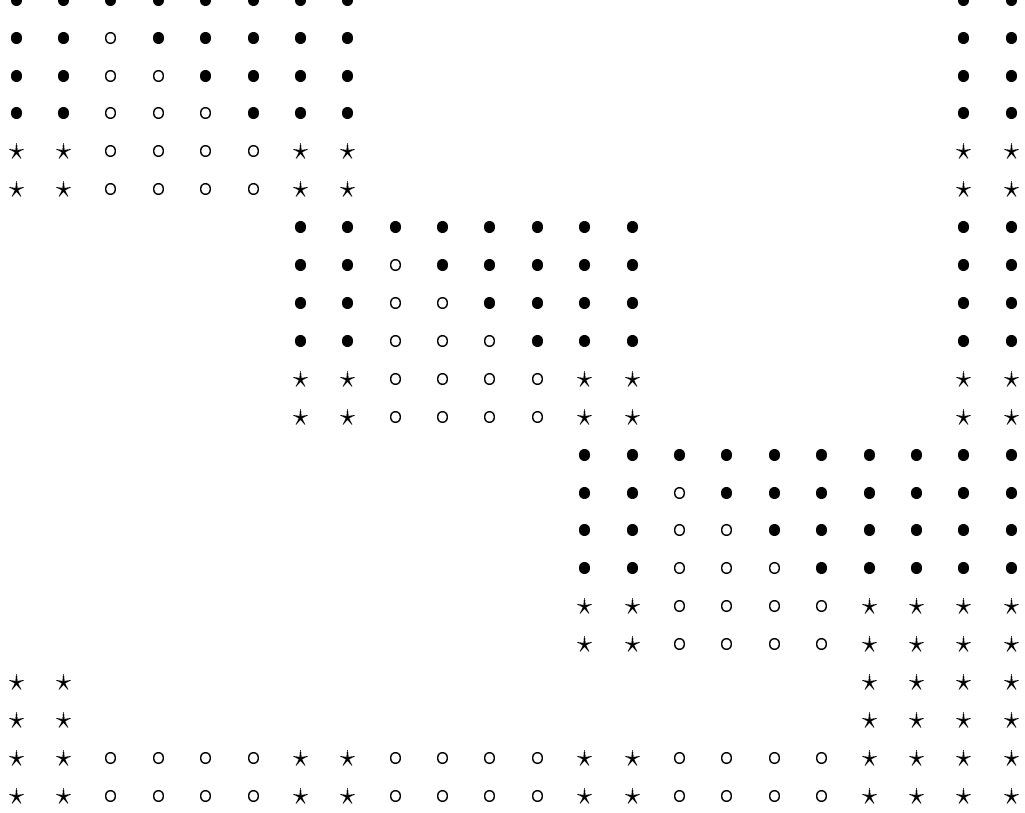

After condensation of parameters.

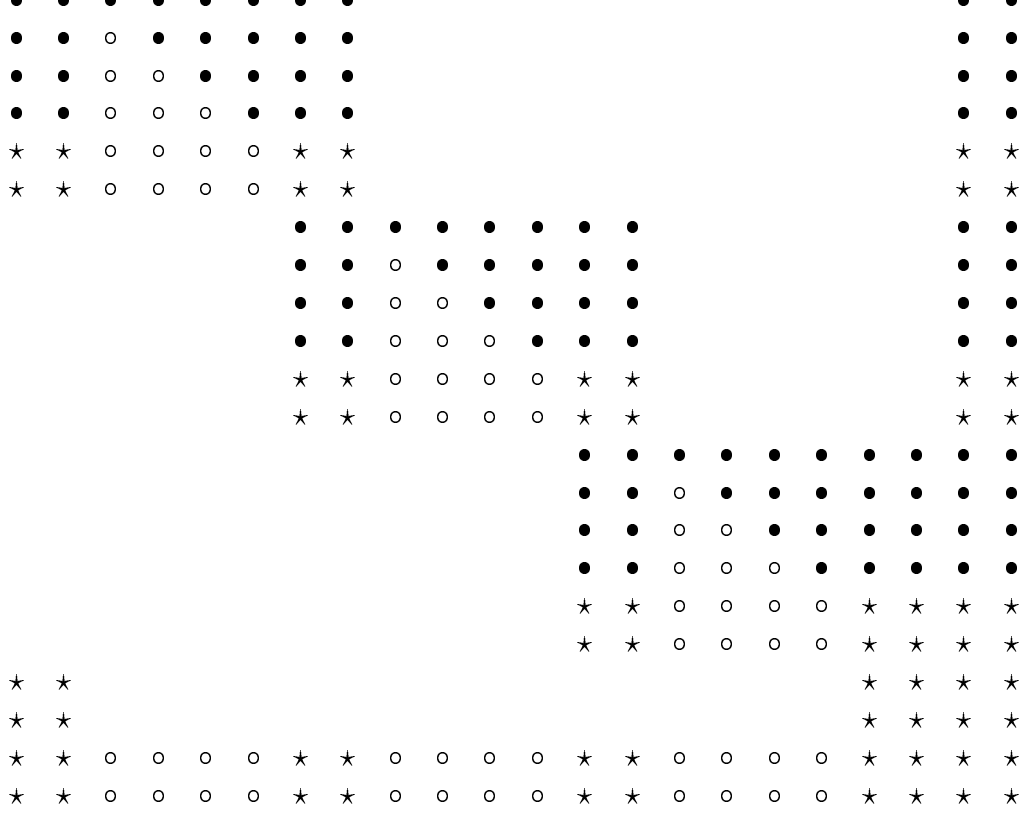

The decoupled system.

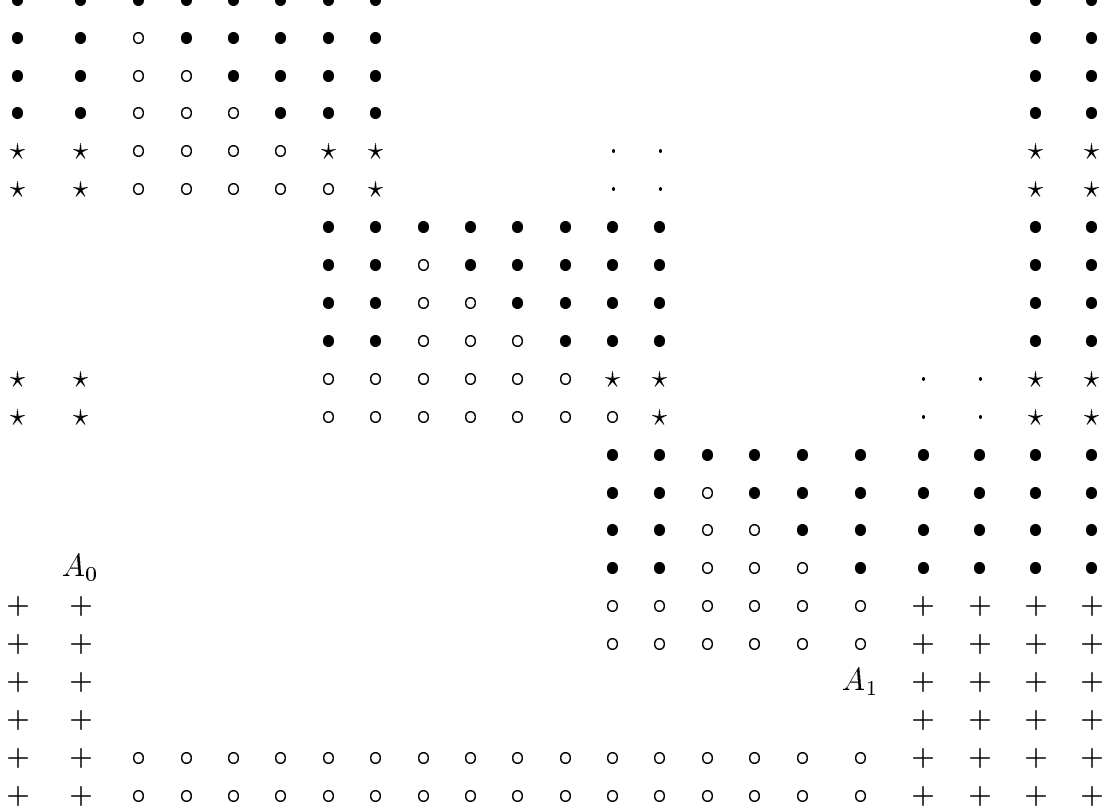

The final reduced system.